MV021 - Globular Ovoid Jar

An Exploration of Precision

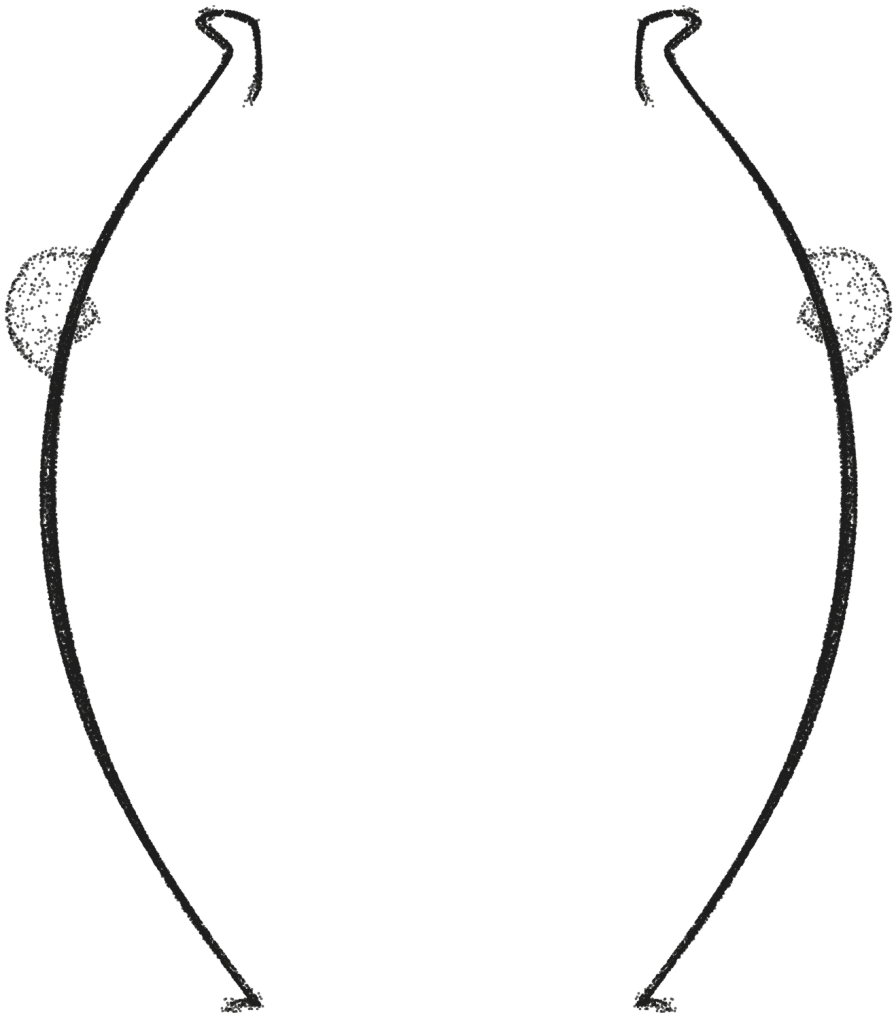

Author: Stine Gerdes, arcsci.org
License: Creative Commons BY-NC-SA 4.0
Date: 2025-03-18
Version: 01.00

Petrie Museum, CC BY-NC-SA

Contents

Artifact Information **2**

Alignment In The Cartesian Coordinate System **3**

Precision **5**
Circularity 5
Concentricity 21
Coaxiality 29
Surface Variability 32
Precision Score Of The Artifact 39

Analysis Roadmap **41**

Appendix A - Comparison Of Circularity Measurements (Z-plane vs. surface-perpendicular) **42**

Appendix B - Comparison Of Concentricity Measurements (Z-plane vs. surface-perpendicular) **49**

Copyright 2025, Stine Gerdes - This work is licensed under CC BY-NC-SA 4.0

Artifact Information

Artifact Data

Collection	Petrie Museum of Egyptian Archaeology
Provenance[1]	Petrie Museum of Egyptian Archaeology (London), recovered by Flinders Petrie
Provenience[2]	Naqada Tomb 1207 (possible Naqada II) - Petrie Excavation
Attribution	(possible) Naqada II

Museum information

Ref.	LDUCE-UC6226
Description	Grey basalt vase with two perforated handles. From Naqada Tomb 1207
URL	https://collections.ucl.ac.uk/Details/collect/13578

Maijers vessel classification[3]

Short classification	Globular Ovoid Jar
Long classification	The vessel is created in a closed form classified as a globular jar with a ovoid shape, a rounded rim.

Physical properties

Precision score[4]	10
Height (approximate)	96 mm 3.78 in
Width (approximate)	77 mm 3.03 in
Material	Grey Basalt
Mohs Hardness[5]	5 - 7 (Basalt)
Weight	

Scan information

Source	Scanned by Artifact Foundation
Source file name	Not specified
Scan method	Laser
Scanner	FreeScale Combo+
Rated scan accuracy	37 µm | 1.51 thou
Scan date	2024-10-07
Scanned by	Adam Young and Károly Póka
Mesh decimation	None, raw scan file used in the analysis
Number of vertices	4 129 411
Mesh density[6]	36 µm | 1.40 thou
Max vertex distance	130 µm | 5.121 thou
Min vertex distance	0 µm | 0.000 thou
Vertices per cm2	19 695 (approximated)
Vertices per in2	127 064 (approximated)

[1] The verifiable chain of custody of an artifact

[2] The location or site where an artifact was recovered

[3] Vessel artifact classification developed by W. Arnold Maijer and described in his publication Masters of Stone, ISBN 978-90-829212-0-5

[4] The precision score metric is described in Precision Score Of The Artifact, p. 40

[5] The Mohs scale is an ordinal scale, from 1 to 10, describing the materials resistance to abrasion (the ability of harder material to scratch softer material)

[6] Median distance between vertices

Copyright 2025, Stine Gerdes - This work is licensed under CC BY-NC-SA 4.0

Alignment In The Cartesian Coordinate System

For precise and valid measurements of the vessel's geometry to be possible, the points of the scanned dataset must first and foremost be placed optimally in a Cartesian coordinate system. Several alignment methods and algorithms have been tested on a number of different vessels to determine the best way to achieve optimal alignment.

Any misalignment of the artifact will increase the error of the precision measurements, due to the distortion/ wobble effect caused by the misaligned object. To visualize this distortion, we can consider a representation of the three-dimensional point cloud data, folded to a two-dimensional plane. This folded representation is obtained by rotating all scanned points around an assumed center axis to $y = 0$, $x > 0$, thus resulting in a two-dimensional profile representation of all scanned vertices in the object.

Figure 1 illustrates this effect on a ideal ellipsoid. In the first image, the ellipsoid is perfectly aligned, resulting in a narrow and precise two-dimensional folded profile. As misalignments are introduced, the two-dimensional profile increases in width, visually showing the distortion, causing the error in the precision measurements to increase. While easy to understand visually, this distortion can also be objectively quantified, and as such used to compare the fitness of different assumed center axes against each other, and further to create an automated and solid process for optimal Cartesian alignment of the scan data.

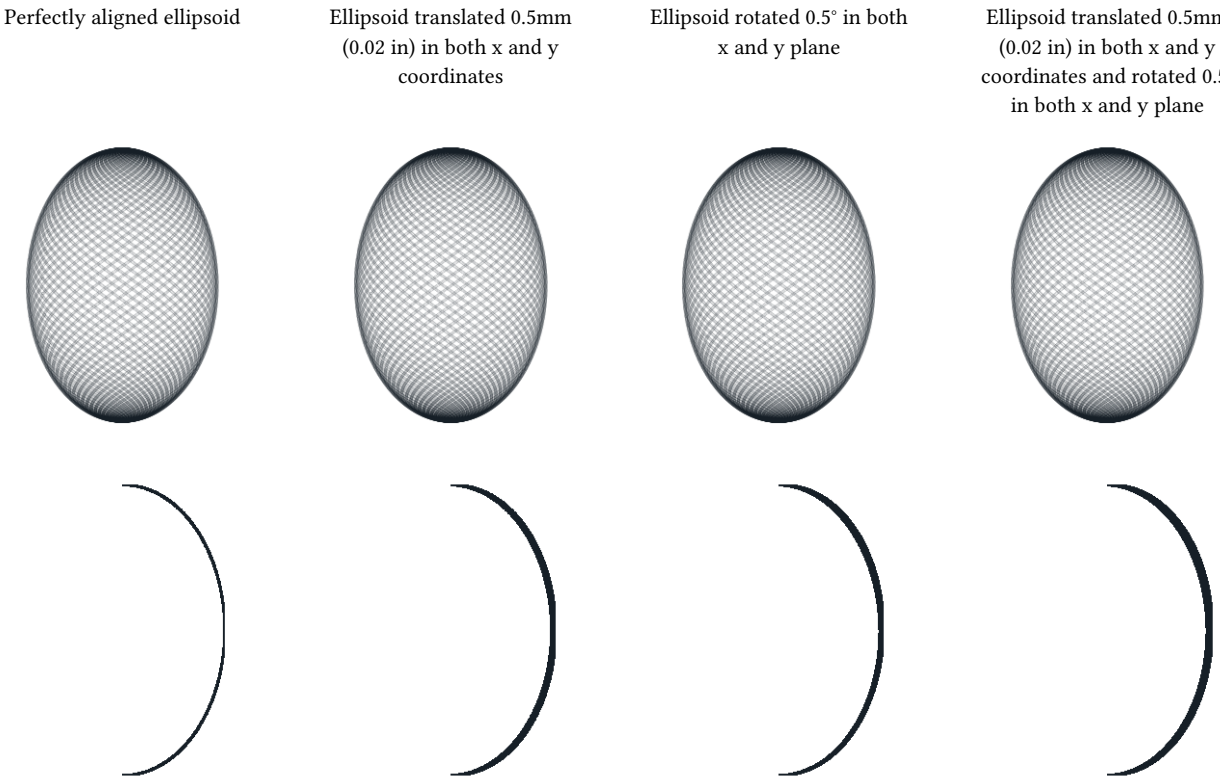

Figure 1: Distortion caused by a misalignment of the artifact

In contemporary metrology analysis of modern production objects, it is common to align the object in a Cartesian coordinate system by fitting a flat surface of the object to a reference plane in the coordinate system, cylindrical features to an ideal cylinder etc., or by using specific markers placed on the object in the design process. This methodology, however, is inadequate for the ancient objects in question. Most scanned artifacts, do not have a valid flat surface which could be aligned to a plane in the Cartesian coordinate system; most surfaces seem to be curved. Some artifacts do have a flat base, however this is often a worn area of the artifact and practical tests have shown that alignment to such surfaces will not produce optimal alignment of the scan data.

As conventional methods of alignment do not always yield good results with these types of artifacts, a more adequate method of alignment has been developed to enable precise measurements and statistical analysis of the scan data.

Copyright 2025, Stine Gerdes - This work is licensed under CC BY-NC-SA 4.0

To find the optimal position of the vessel in the coordinate system, a range of rotation and translation tests are carried out to find the best fit of the central axis.

Based on the assumption that the analyzed object was created using a rotational process, and thus have symmetry around a central axis, the alignment of the artifact is carried out in a two-step process. An overview of this process is given below.

The artifact is placed in a Cartesian coordinate system, in an initially unaligned state. The first step in the alignment process estimates the central rotational axis of the vessel, by analyzing the coaxiality of thin cross-section slices of the vessel. The slices will be as thin as possible based on the mesh density of the scan, while still ensuring enough data points in each slice to be statistically valid.

For each slice, circular regression[7] (estimate of best fit circle) is used to estimate the center point of this slice. Combined over the total Z-axis range of the vessel, these center points provide us with an indicator of the incline and position of the vessel's central axis.

The next step will optimize the center axis alignment by progressively minimizing the deviation (perpendicular to the surface curvature) of the two-dimensional profile, see Figure 1. By ascertaining and comparing the resulting fit of many thousands of different potential rotations, the best fit alignment of the scan data can be estimated, and an optimal center axis (in relation to the data points) can be reconstructed. The actual three-dimensional point-cloud is then aligned to this axis, by rotating and translating the scanned data points to match the Z-axis of the Cartesian coordinate system.

[7] Circle regression algorithm used: Kenichi Kanatani, Prasanna Rangarajan, "Hyper least squares fitting of circles and ellipses" Computational Statistics & Data Analysis, Vol. 55, pages 2197-2208, (2011)

Copyright 2025, Stine Gerdes - This work is licensed under CC BY-NC-SA 4.0

Precision

To explore the manufacturing precision of the artifact in depth, the following analysis have been carried out:

- Circularity around the axis of symmetry is examined in detail at selected cross-sections.
- Overall circularity around the axis of symmetry is measured for the full height of the vessel (areas of the vessel with extensive damage are not taken into account for this metric).
- Concentricity of the vessel between selected cross-sections are examined in detail to determine if the existence of an axis of rotation in the manufacture of the object can be established.
- The coaxiality of the vessel is analyzed to explore the precision of the central axis of the object.
- The surface variability is analyzed and visualized on through a heatmap.

Circularity

Circularity is the measurement of how round the surface of an object is, optionally in reference to a datum axis. The *circularity tolerance* is the radial distance of two circles, each with their centers in the datum axis, and each of them conforming, respectively, to the minimum and maximum deviations of the data-set to a true circle, see Figure 2.

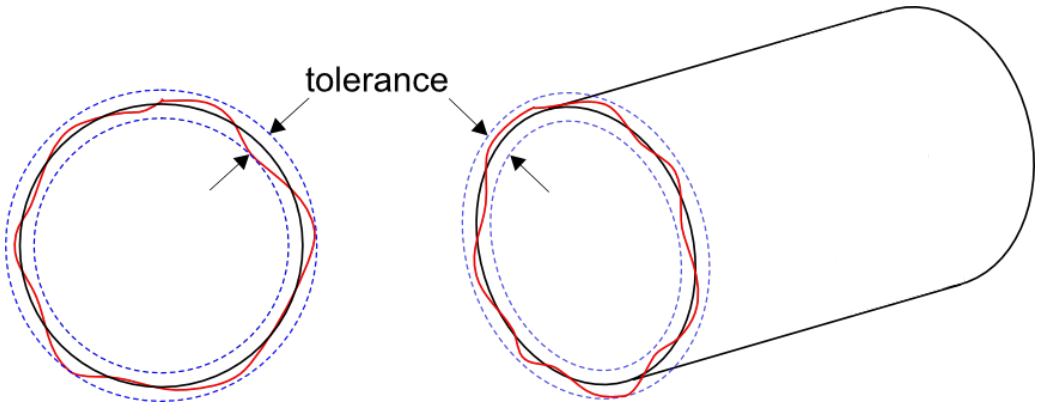

Figure 2: Circularity tolerance.

Circularity is examined at different cross-sections of the vessel, using the established Z-axis as the datum axis (axis of symmetry). The distance between the scanned points in the local datum plane is measured to determine the range between the two concentric circles encompassing the measured points, see Figure 3.

Referencing all of the individual circularity measurements to the global (reconstructed) axis of symmetry of the object, allows us to ascertain not only circularity of local features of the object, but how well circularity was *maintained* over the entire manufacturing process. This is an important distinction, which may be able to provide valuable insights into requirements of the construction methods. For reference, and seeing that the variance in local circularity also holds interest, measurements of circularity of the vessel without reference to the axis of symmetry can additionally be found in the Concentricity, p. 22.

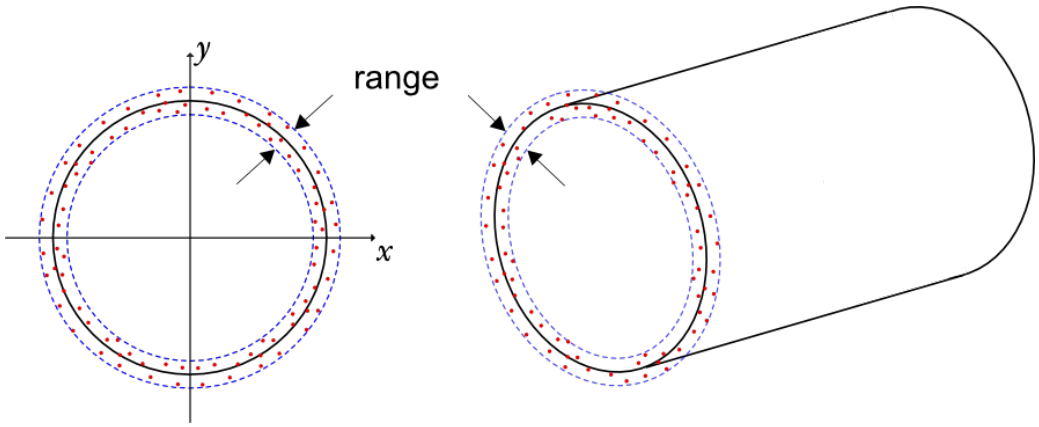

Figure 3: Circularity measurements.

Copyright 2025, Stine Gerdes - This work is licensed under CC BY-NC-SA 4.0

If the circularity is determined from slices of the vessel exclusively in the *Z-plane* (actually measuring the cylindricity of a very thin slices of the vessel, in an attempt to approximate circularity), this would - in some areas - introduce significant distortion (increasing measurement errors) in the samples, due to the curvature of the vessel's surface.

Each sample slice of the vessel is therefore obtained perpendicular to the surface curvature, see Figure 5 to Figure 10. The measurements are taken conservatively without filtration of potential outliers.

To explore the potential distortion caused by obtaining samples in the Z-plane only, please refer to Appendix A, where measurements in the Z-plane and measurements perpendicular to surface curvature are compared side by side.

Detailed circularity measurements of selected points

Circularity measurements across a range of selected slices of the vessel (see Table 1) have been analyzed in-depth, and detailed plots of each measurement is provided. Furthermore, full circularity measurements are shown for each available scanned surface including a detailed plot to visualize the circularity of all areas of the vessel.

Copyright 2025, Stine Gerdes - This work is licensed under CC BY-NC-SA 4.0

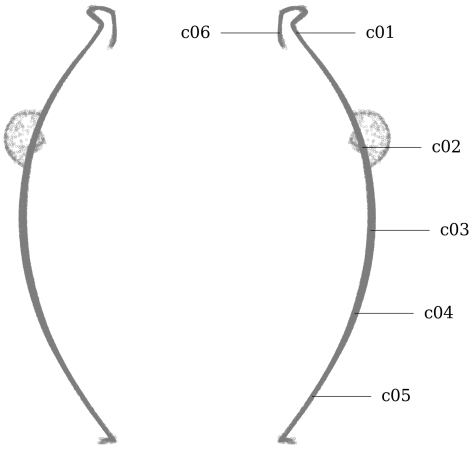

Figure 4: Circularity measurement sample location on MV021.

Metric

Tag	Area	Measured deviation[8]	Residuals				Sample size	Slice		
			Range	RMSD[9]	MAD[10]	SD		Height	Z coord.	Radius[11]
		mm	mm	mm	mm	mm		mm	mm	mm
c01	exterior	Ø43.185±0.307	0.531	0.139	0.119	0.139	1079	0.050	88.734	21.593
c02	exterior	Ø71.861±0.591	1.089	0.332	0.320	0.332	1682	0.050	63.941	35.931
c03	exterior	Ø75.456±0.819	1.464	0.451	0.421	0.451	2236	0.050	45.954	37.728
c04	exterior	Ø68.488±0.596	1.159	0.358	0.323	0.358	1889	0.050	27.968	34.244
c05	exterior	Ø50.051±0.387	0.742	0.181	0.143	0.181	1134	0.050	9.981	25.026
c06	interior	Ø35.924±0.424	0.690	0.169	0.151	0.169	985	0.050	88.734	17.962

Imperial

Tag	Area	Measured deviation[8]	Residuals				Sample size	Slice		
			Range	RMSD[9]	MAD[10]	SD		Height	Z coord.	Radius[11]
		in	in	in	in	in		in	in	in
c01	exterior	Ø1.7002±0.0121	0.0209	0.0055	0.0047	0.0055	1079	0.0020	3.4935	0.8501
c02	exterior	Ø2.8292±0.0233	0.0429	0.0131	0.0126	0.0131	1682	0.0020	2.5173	1.4146
c03	exterior	Ø2.9707±0.0322	0.0576	0.0177	0.0166	0.0177	2236	0.0020	1.8092	1.4854
c04	exterior	Ø2.6964±0.0235	0.0456	0.0141	0.0127	0.0141	1889	0.0020	1.1011	1.3482
c05	exterior	Ø1.9705±0.0152	0.0292	0.0071	0.0056	0.0071	1134	0.0020	0.3930	0.9853
c06	interior	Ø1.4143±0.0167	0.0272	0.0066	0.0059	0.0066	985	0.0020	3.4935	0.7072

Table 1: Detailed circularity measurements at selected samples of MV021.

Figure 5 to Figure 10 shows a detailed plots of each circularity measurement.

[8]Sample diameter Ø± maximum measured deviation from measured radius
[9]Root mean square deviation (RMSD) also called Root mean square error (RMSE)
[10]Median absolute deviation
[11]Median sample radius from z-axis

Copyright 2025, Stine Gerdes - This work is licensed under CC BY-NC-SA 4.0

Graphical overview of circularity measurement c01

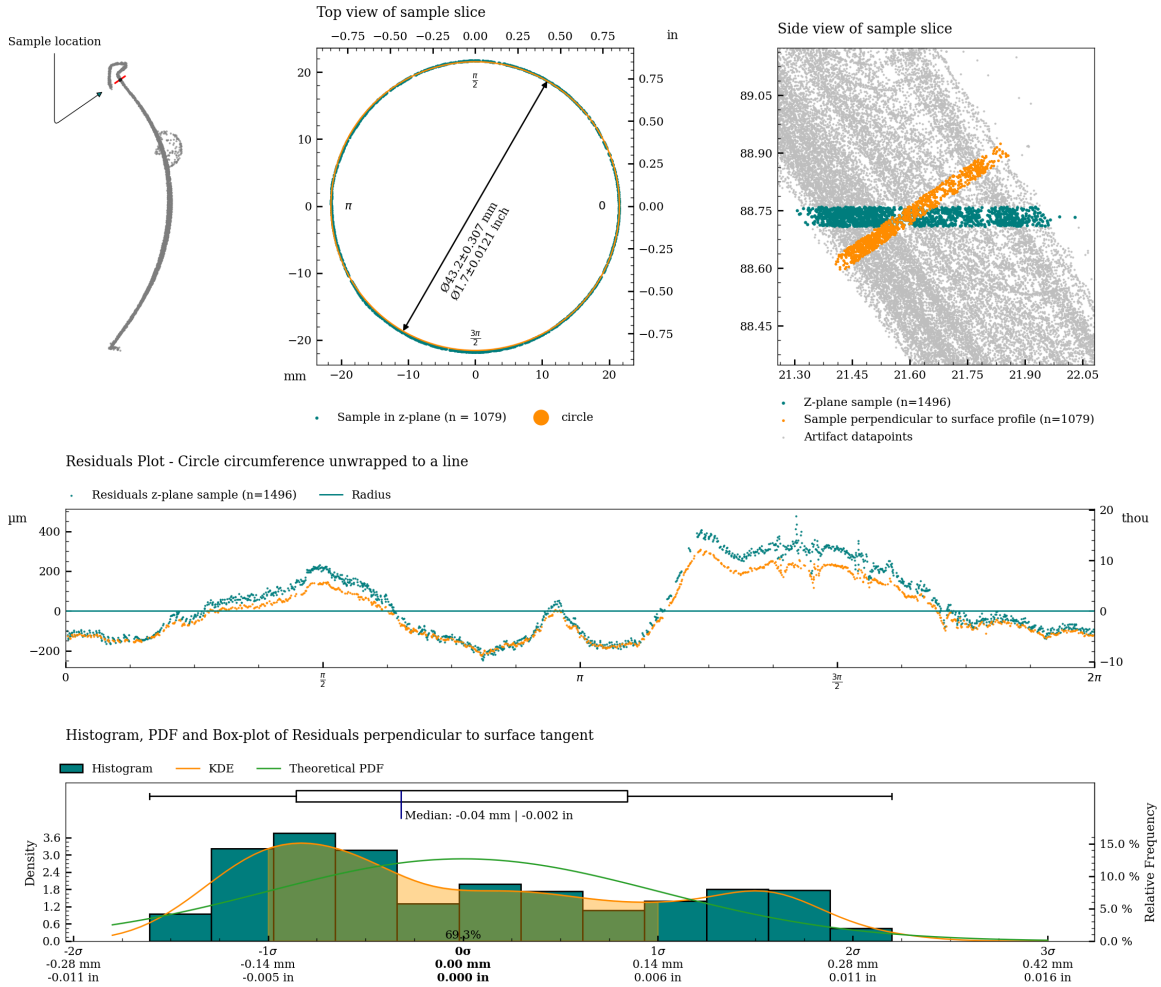

Figure 5: Charts with statistics for the measurement of c01.

Copyright 2025, Stine Gerdes - This work is licensed under CC BY-NC-SA 4.0

Graphical overview of circularity measurement c02

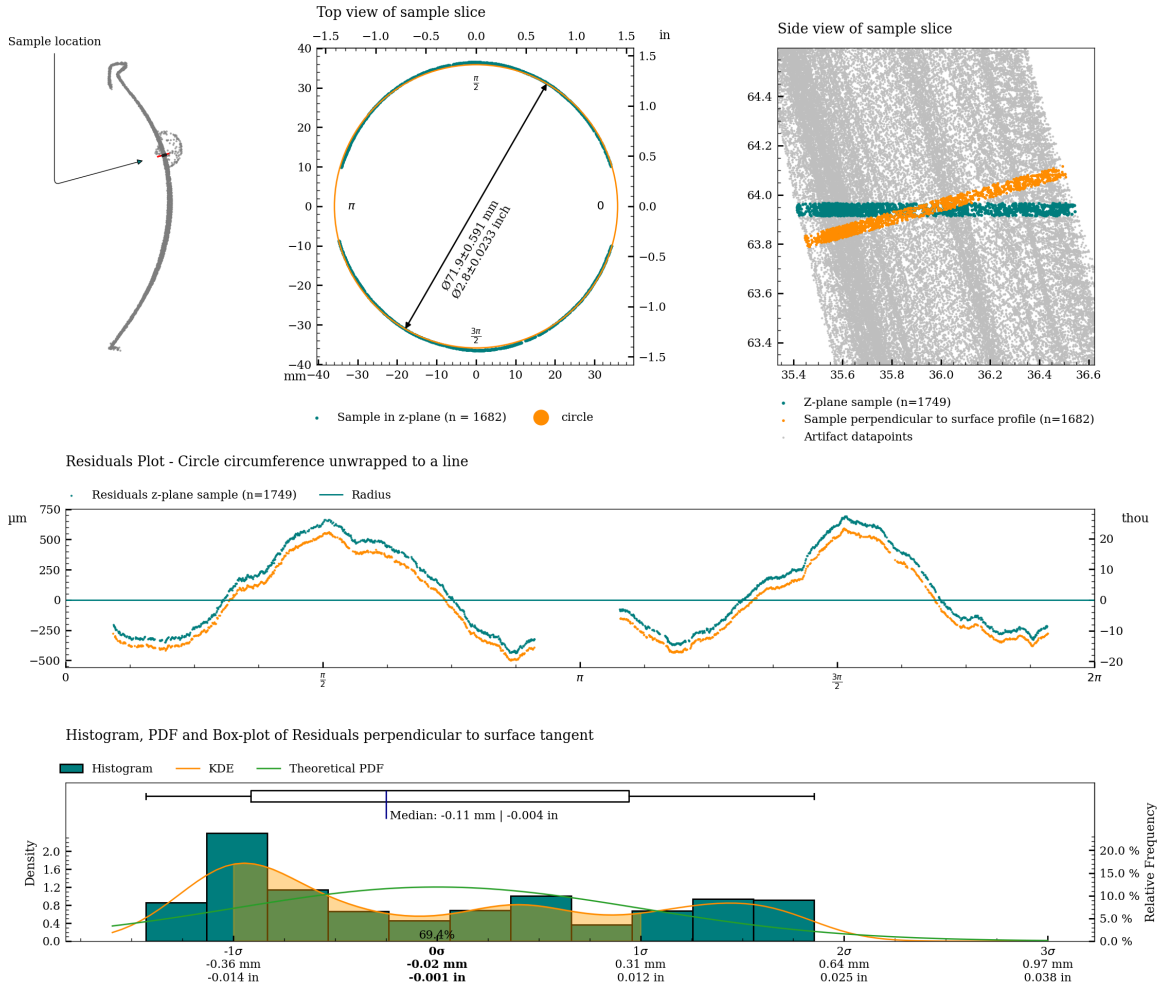

Figure 6: Charts with statistics for the measurement of c02.

Copyright 2025, Stine Gerdes - This work is licensed under CC BY-NC-SA 4.0

Graphical overview of circularity measurement c03

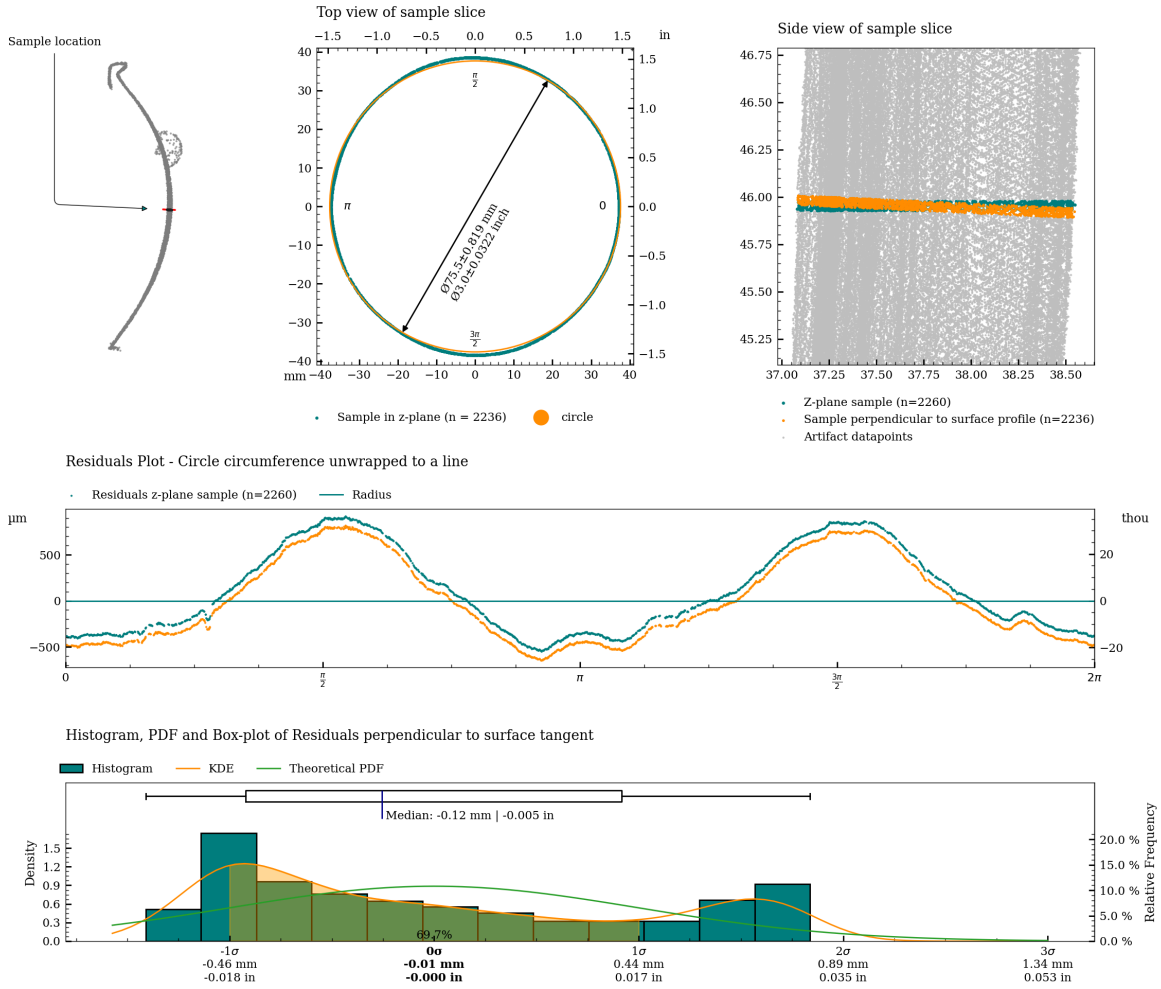

Figure 7: Charts with statistics for the measurement of c03.

Copyright 2025, Stine Gerdes - This work is licensed under CC BY-NC-SA 4.0

Graphical overview of circularity measurement c04

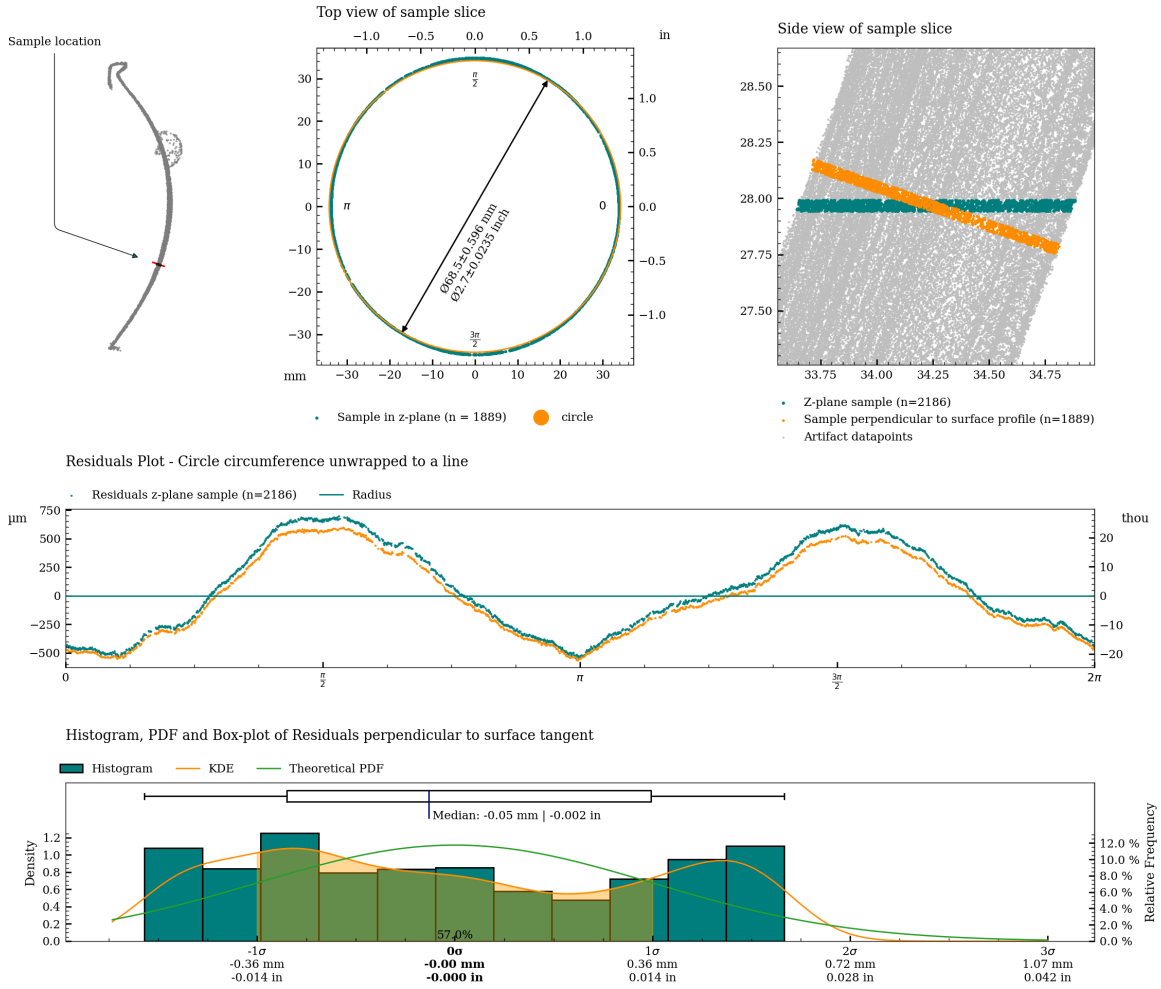

Figure 8: Charts with statistics for the measurement of c04.

Copyright 2025, Stine Gerdes - This work is licensed under CC BY-NC-SA 4.0

Graphical overview of circularity measurement c05

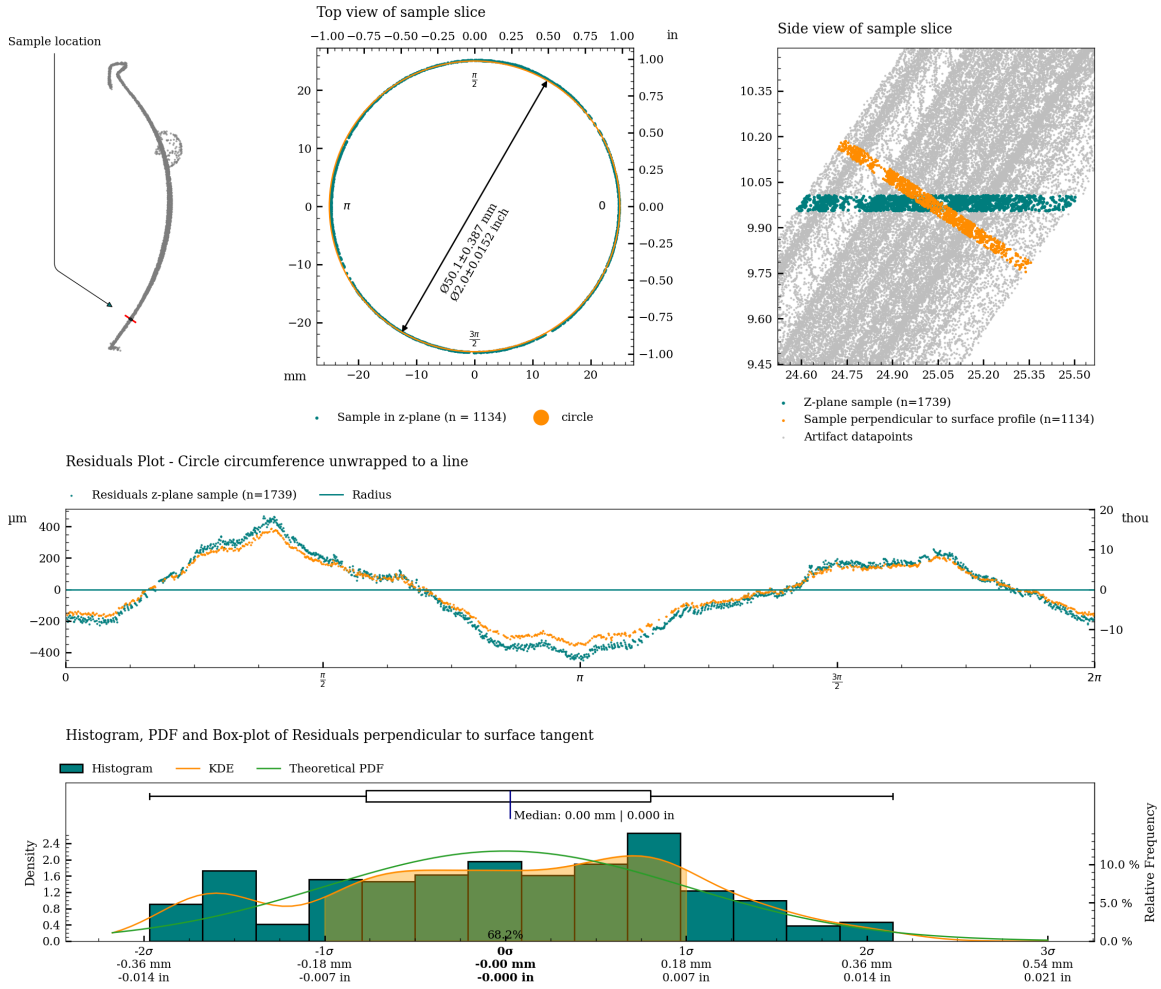

Figure 9: Charts with statistics for the measurement of c05.

Copyright 2025, Stine Gerdes - This work is licensed under CC BY-NC-SA 4.0

Graphical overview of circularity measurement c06

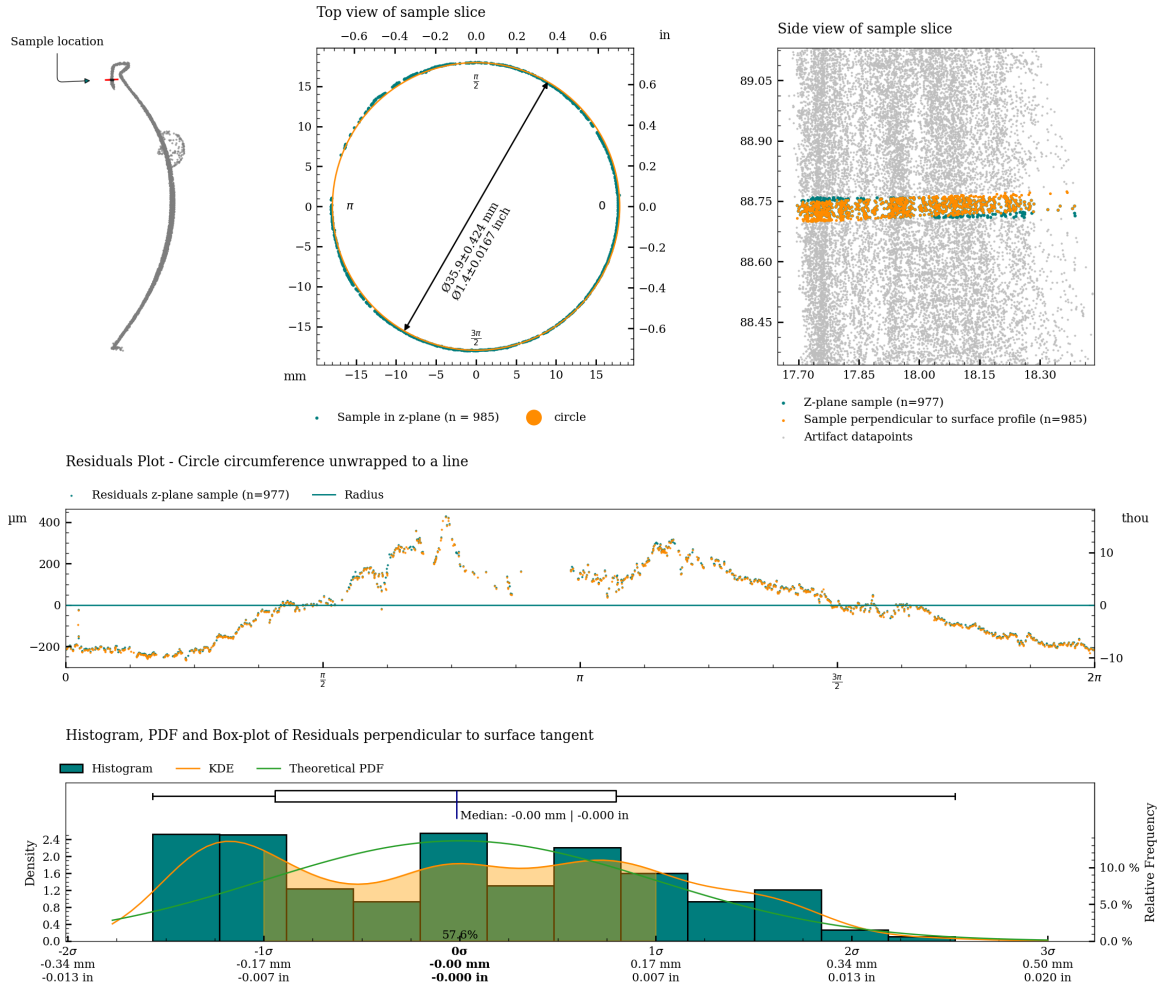

Figure 10: Charts with statistics for the measurement of c06.

Copyright 2025, Stine Gerdes - This work is licensed under CC BY-NC-SA 4.0

Table 2 shows statistical measures of the circularity of the vessel, measured along the full height (damaged parts may reduce the measurement area).

Metric

Area	Range			Standard Deviation			Medan Absolute Deviation			Slices	Slice height
	Median	Min.	Max.	Median	Min.	Max.	Median	Min.	Max.		
	mm	mm	mm	mm	mm	mm	mm	mm	mm		mm
Exterior	0.977	0.426	1.467	0.299	0.109	0.458	0.074	0.059	0.373	1800	0.050
Interior	0.643	0.430	1.231	0.166	0.115	0.291	0.027	0.073	0.197	165	0.050

Imperial

Area	Range			Standard Deviation			Medan Absolute Deviation			Slices	Slice height
	Median	Min.	Max.	Median	Min.	Max.	Median	Min.	Max.		
	in	in	in	in	in	in	in	in	in		in
Exterior	0.977	0.426	1.467	0.299	0.109	0.458	0.074	0.059	0.373	1800	0.050
Interior	0.643	0.430	1.231	0.166	0.115	0.291	0.027	0.073	0.197	165	0.050

Table 2: Perpendicular Circularity analysis of MV021.

Copyright 2025, Stine Gerdes - This work is licensed under CC BY-NC-SA 4.0

Circularity analysis of exterior surface

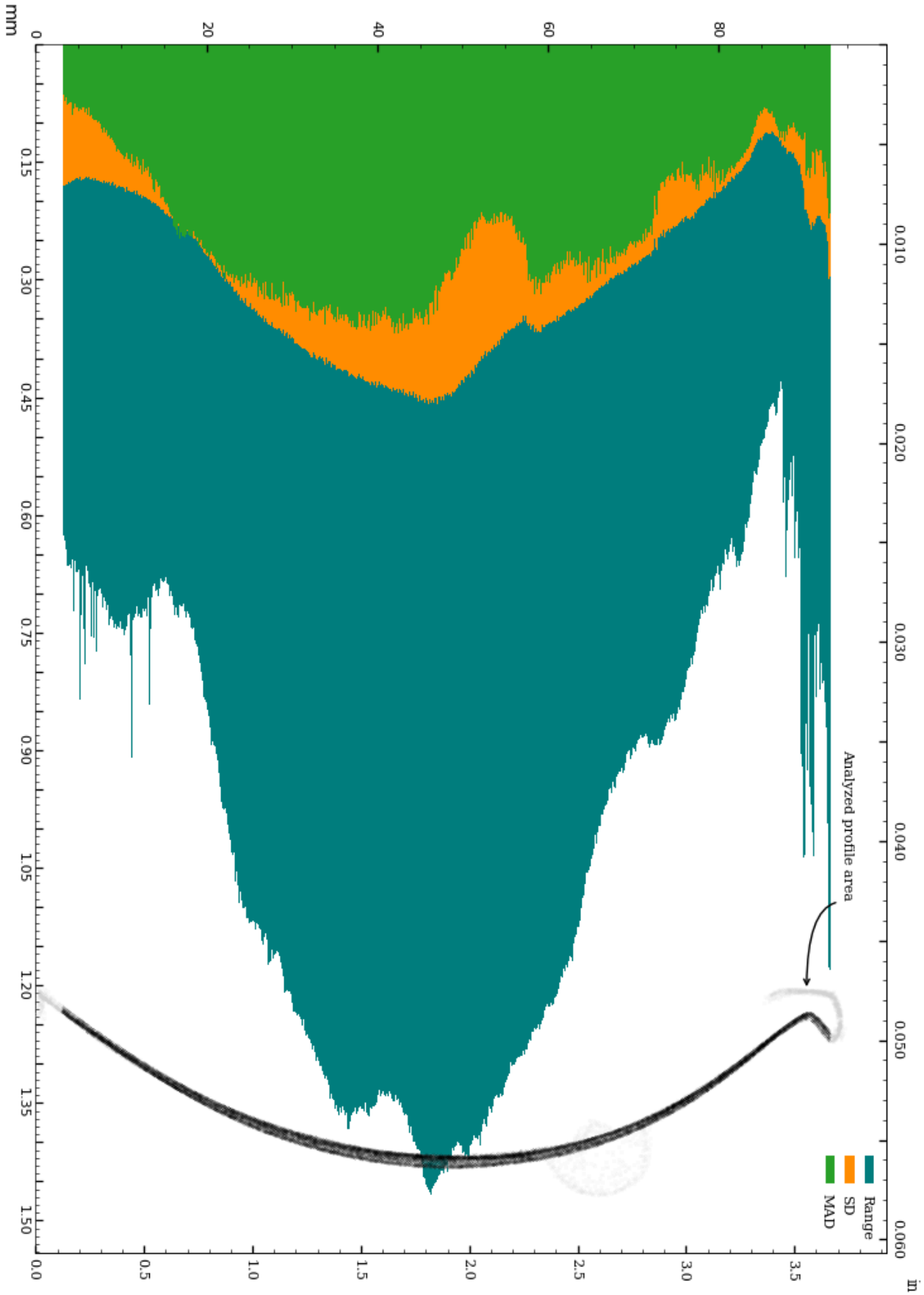

Figure 11: Circularity of exterior surface.

Copyright 2025, Stine Gerdes - This work is licensed under CC BY-NC-SA 4.0

Circularity analysis of exterior surface, Standard Deviation and Median Absolute Deviation

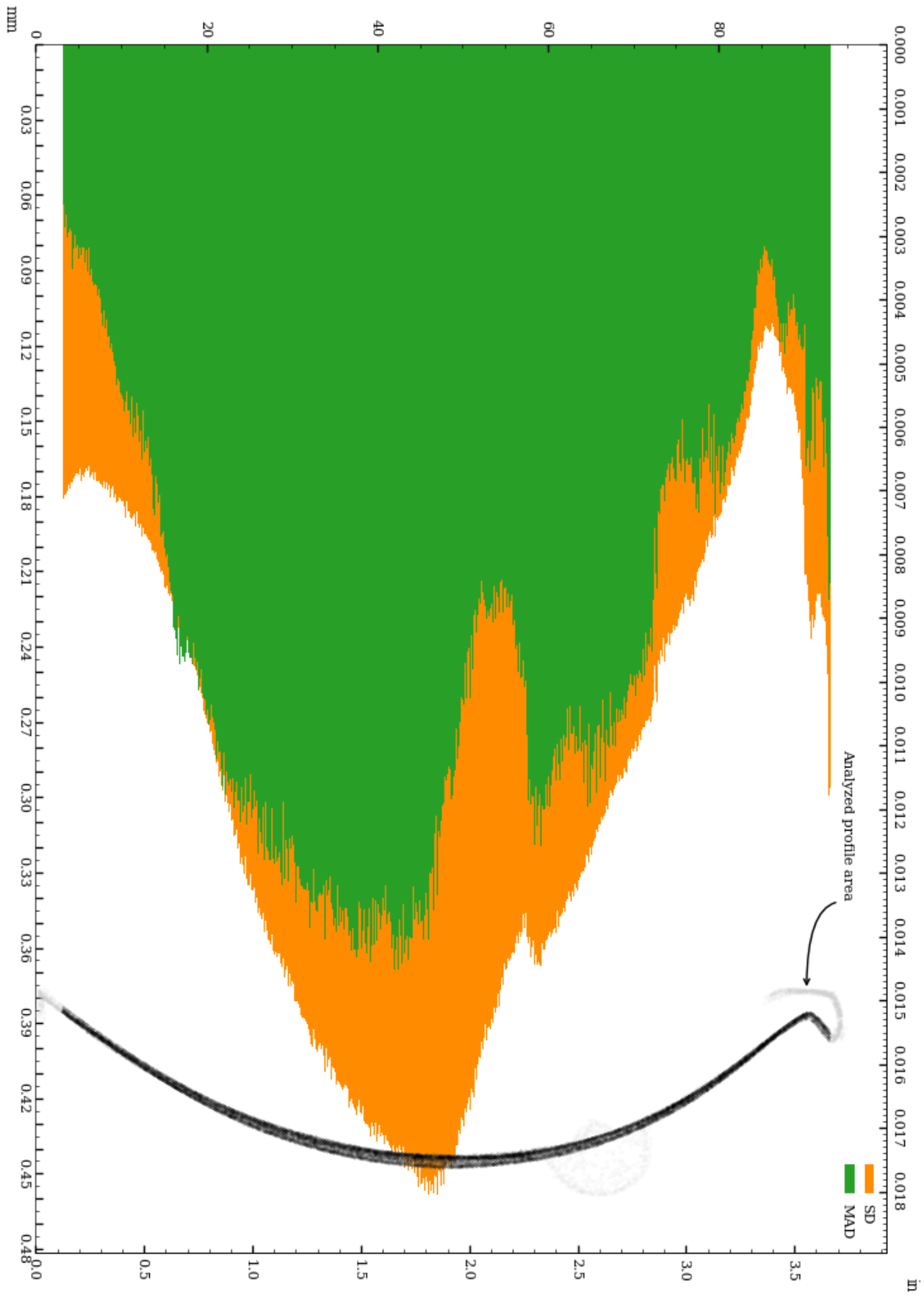

Figure 12: Vessel circularity of exterior surface, standard deviation and median absolute deviation.

Copyright 2025, Stine Gerdes - This work is licensed under CC BY-NC-SA 4.0

The distributions of the circularity measurements across 1800 slices of the exterior surface are shown below.

Range measurement distribution across 1800 slices of exterior surface

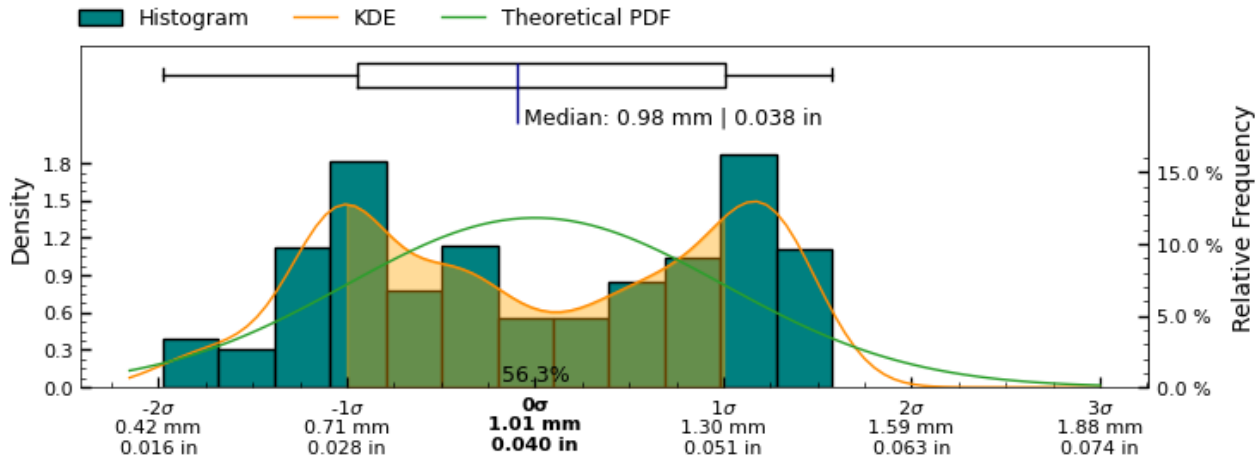

Figure 13: Range measurement distribution across measured slices of exterior surface

Standard deviation measurement distribution across 1800 slices of exterior surface

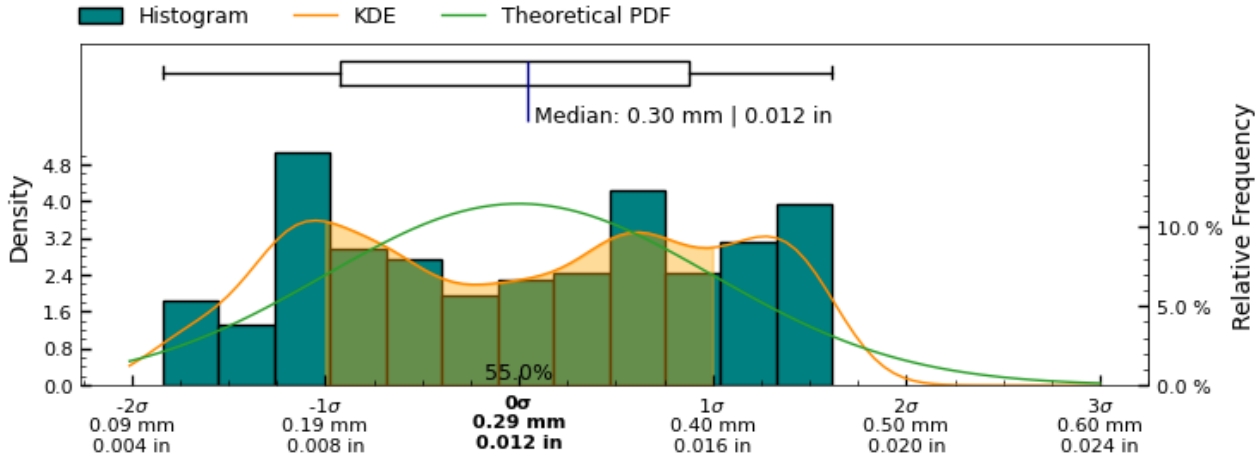

Figure 14: Standard deviation measurement distribution across measured slices of “ + exterior + “ surface

Median absolute deviation measurement distribution across 1800 slices of exterior surface

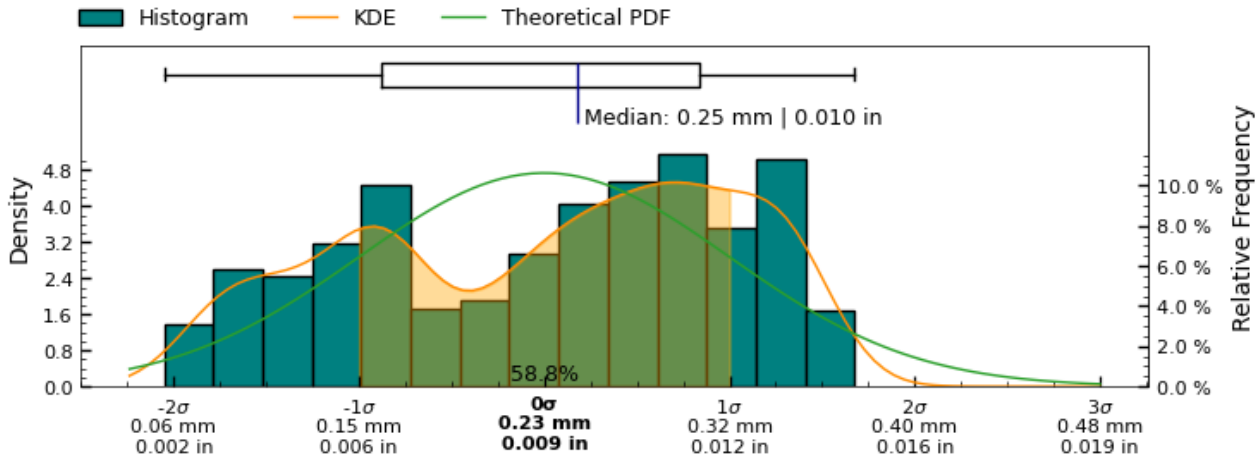

Figure 15: Median absolute deviation measurement distribution across measured slices of exterior surface

Copyright 2025, Stine Gerdes - This work is licensed under CC BY-NC-SA 4.0

Circularity analysis of interior surface

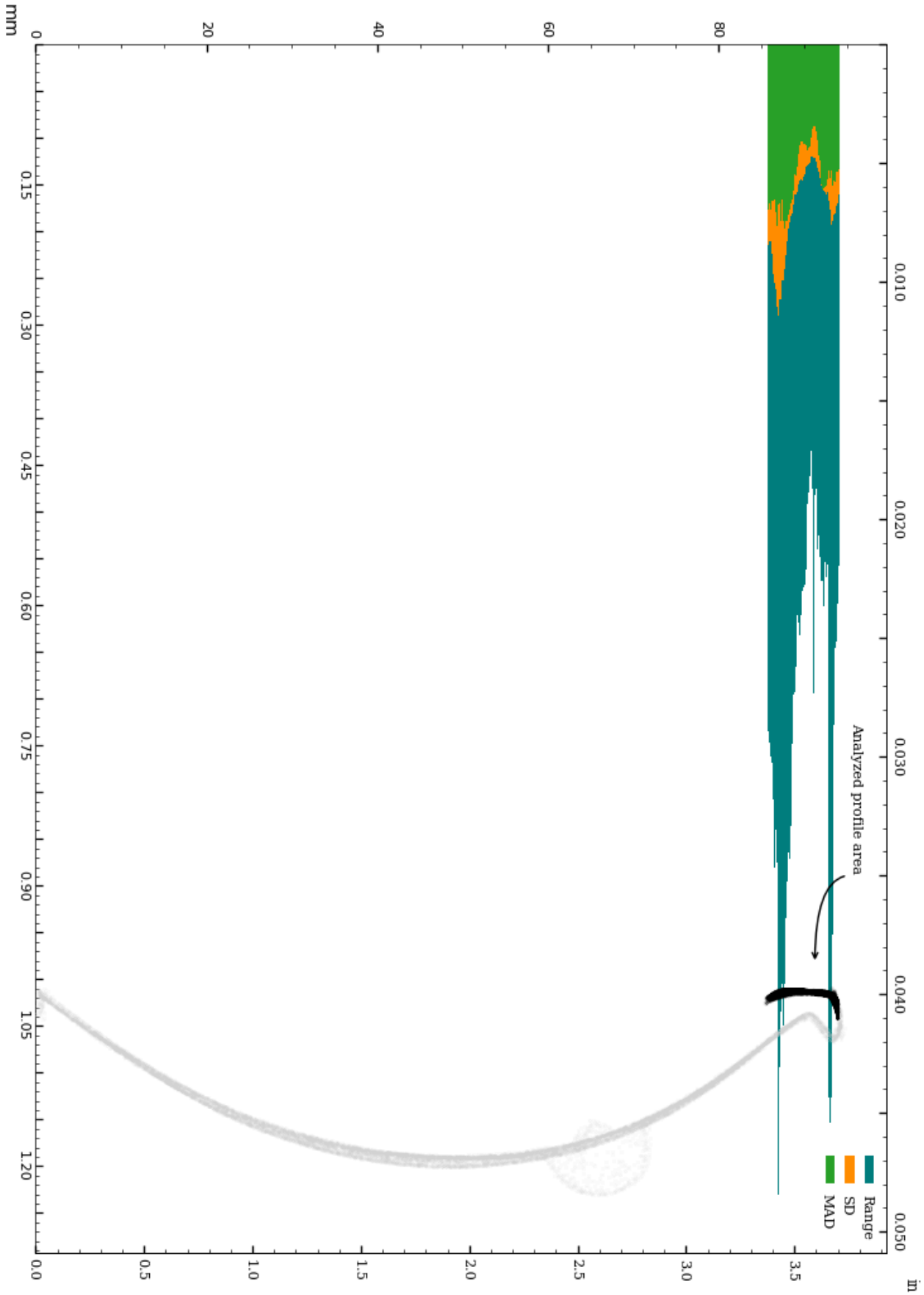

Figure 16: Circularity of interior surface.

Copyright 2025, Stine Gerdes - This work is licensed under CC BY-NC-SA 4.0

Circularity analysis of interior surface, Standard Deviation and Median Absolute Deviation

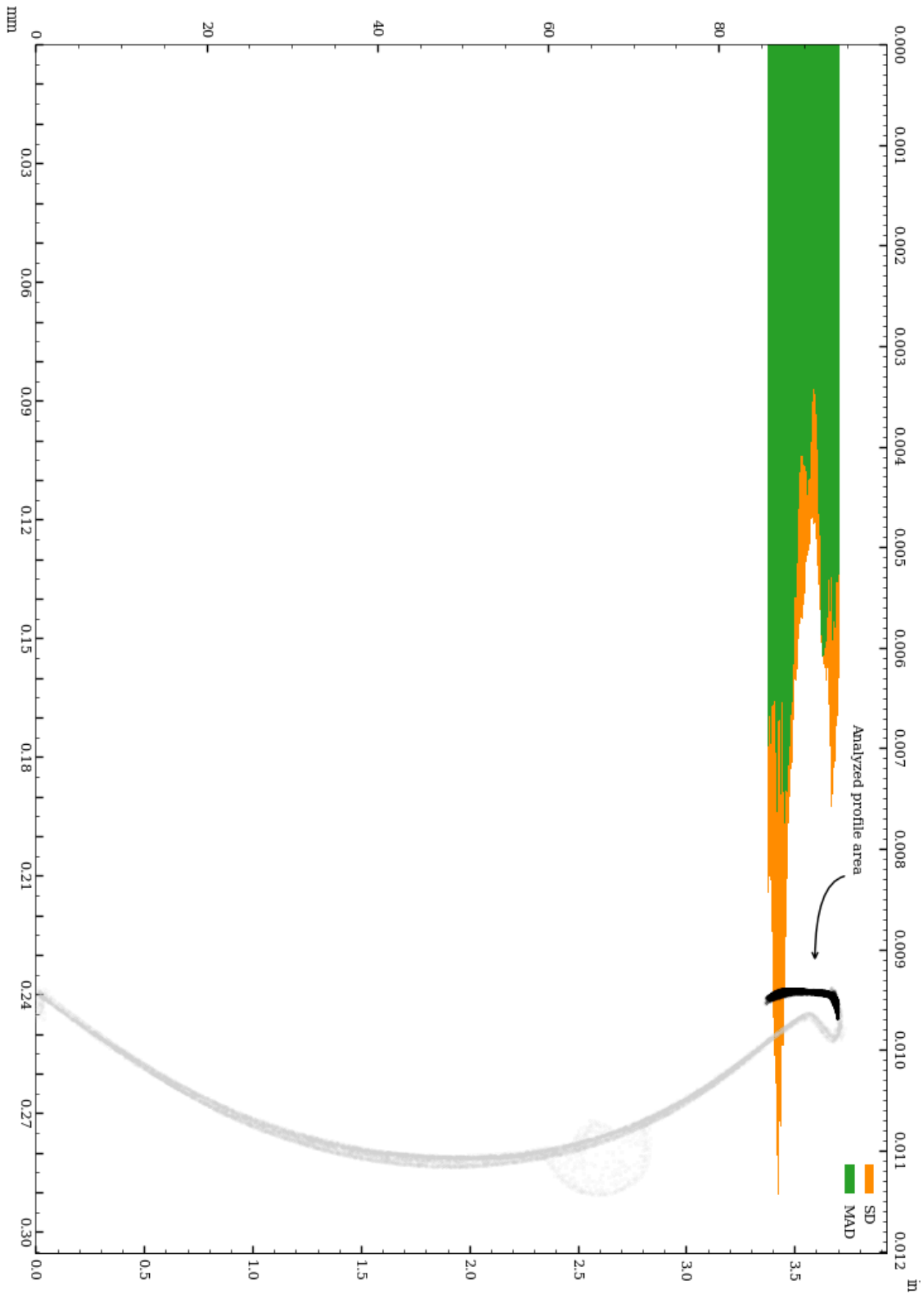

Figure 17: Vessel circularity of interior surface, standard deviation and median absolute deviation.

Copyright 2025, Stine Gerdes - This work is licensed under CC BY-NC-SA 4.0

The distributions of the circularity measurements across 165 slices of the interior surface are shown below.

Range measurement distribution across 165 slices of interior surface

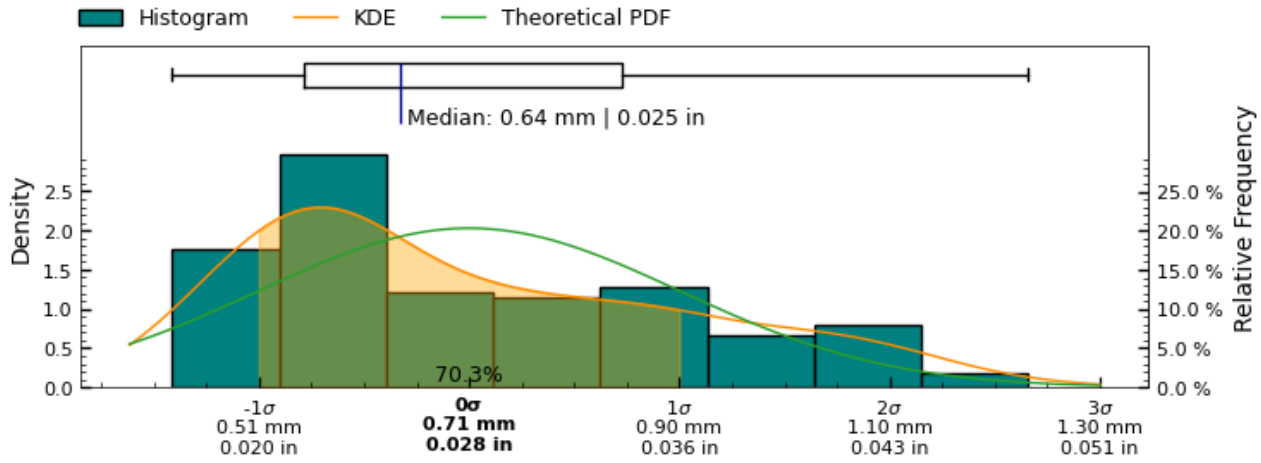

Figure 18: Range measurement distribution across measured slices of interior surface

Standard deviation measurement distribution across 165 slices of interior surface

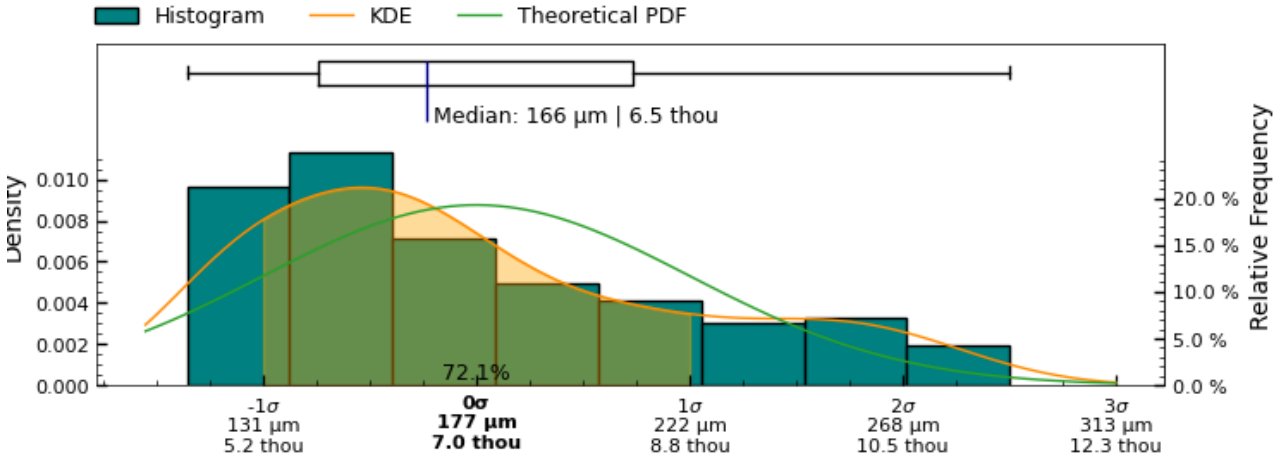

Figure 19: Standard deviation measurement distribution across measured slices of “ + interior + “ surface

Median absolute deviation measurement distribution across 165 slices of interior surface

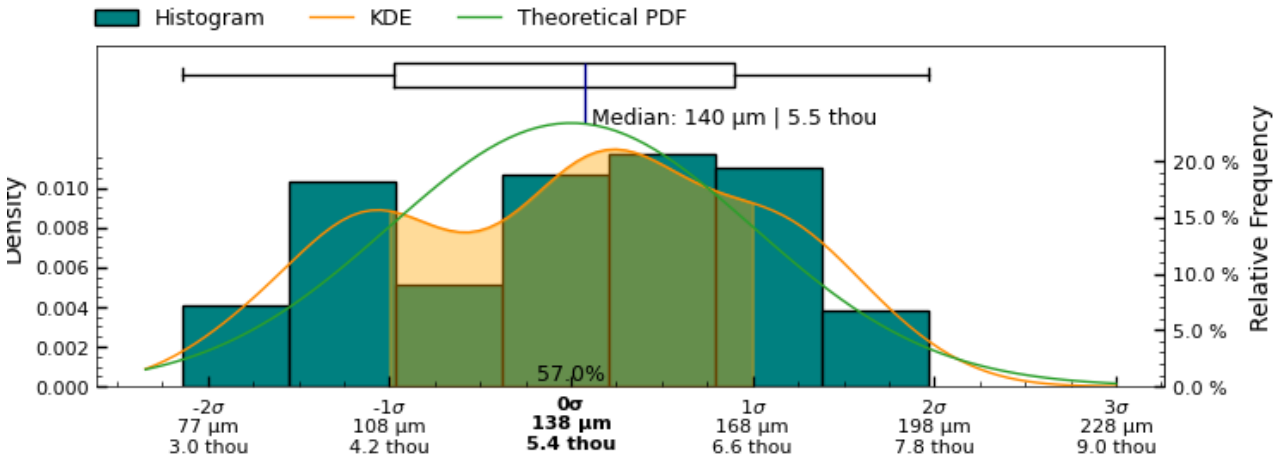

Figure 20: Median absolute deviation measurement distribution across measured slices of interior surface

Copyright 2025, Stine Gerdes - This work is licensed under CC BY-NC-SA 4.0

Concentricity

The concentricity metric describes the deviation in the center-point of the referenced features. As such, it is a measure to determine if several features of the object share the same center point/axis, and how closely. See Figure 21 for a visual representation of this metric.

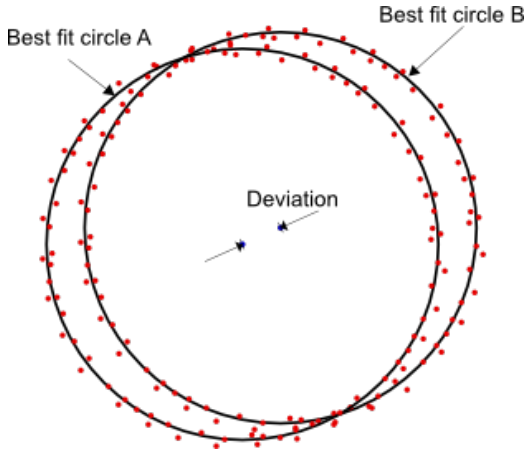

Figure 21: Concentricity measures the deviation (distance) between the center of two circles.

Determination of concentricity has been carried out by establishing the best fit circles of sample slices, using RANSAC (Random sample consensus) algorithm for outlier detection of a least squares circle regression on the scanned data-points at each cross-section, to estimate centers of each cross-section.

The concentricity between both the interior and exterior circular cross-sections is explored for cross-section measurements with the same Z-coordinates.

Additionally, the concentricity between each cross-section measurement defined in Figure 4 and the datum axis $(x, y) = (0, 0)$ has been calculated to establish the deviation of the feature center from the datum axis.

Copyright 2025, Stine Gerdes - This work is licensed under CC BY-NC-SA 4.0

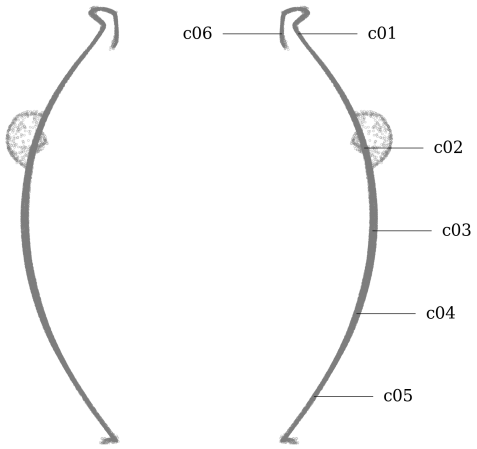

Figure 22: Concentricity measurement sample location on MV021.

Metric

Tag	Reference	Deviation	Sample size	Circle fit residuals analysis for sample listed in Tag column						
				Range full	Range inliers	SD full	SD inliers	MAD full	MAD inliers	Center (x,y)
		mm		mm	mm	mm	mm	mm	mm	µm
c01	z-axis	0.076	1079	0.531	0.531	0.139	0.139	0.100	0.100	−17, −74
c02	z-axis	0.028	1688	1.089	1.089	0.331	0.331	0.251	0.251	17, 22
c03	z-axis	0.020	2233	1.464	1.464	0.450	0.450	0.331	0.331	3, −19
c04	z-axis	0.025	1891	1.159	1.159	0.358	0.358	0.313	0.313	−14, 21
c05	z-axis	0.112	1134	0.742	0.742	0.181	0.181	0.143	0.143	108, 32
c06	z-axis	0.223	985	0.690	0.581	0.169	0.161	0.149	0.146	−222, −13
c01	c06	0.214	1079	0.531	0.531	0.139	0.139	0.100	0.100	205, −61

Imperial

Tag	Reference	Deviation	Sample size	Circle fit residuals analysis for sample listed in Tag column						
				Range full	Range inliers	SD full	SD inliers	MAD full	MAD inliers	Center (x,y)
		in		in	in	in	in	in	in	thou
c01	z-axis	0.0030	1079	0.0209	0.0209	0.0055	0.0055	0.0039	0.0039	−0.7, −2.9
c02	z-axis	0.0011	1688	0.0429	0.0429	0.0131	0.0131	0.0099	0.0099	0.7, 0.9
c03	z-axis	0.0008	2233	0.0576	0.0576	0.0177	0.0177	0.0130	0.0130	0.1, −0.8
c04	z-axis	0.0010	1891	0.0456	0.0456	0.0141	0.0141	0.0123	0.0123	−0.5, 0.8
c05	z-axis	0.0044	1134	0.0292	0.0292	0.0071	0.0071	0.0056	0.0056	4.2, 1.3
c06	z-axis	0.0088	985	0.0272	0.0229	0.0066	0.0063	0.0059	0.0057	−8.8, −0.5
c01	c06	0.0084	1079	0.0209	0.0209	0.0055	0.0055	0.0039	0.0039	8.1, −2.4

Table 3: Concentricity analysis of MV021.

Copyright 2025, Stine Gerdes - This work is licensed under CC BY-NC-SA 4.0

Concentricity analysis of c01

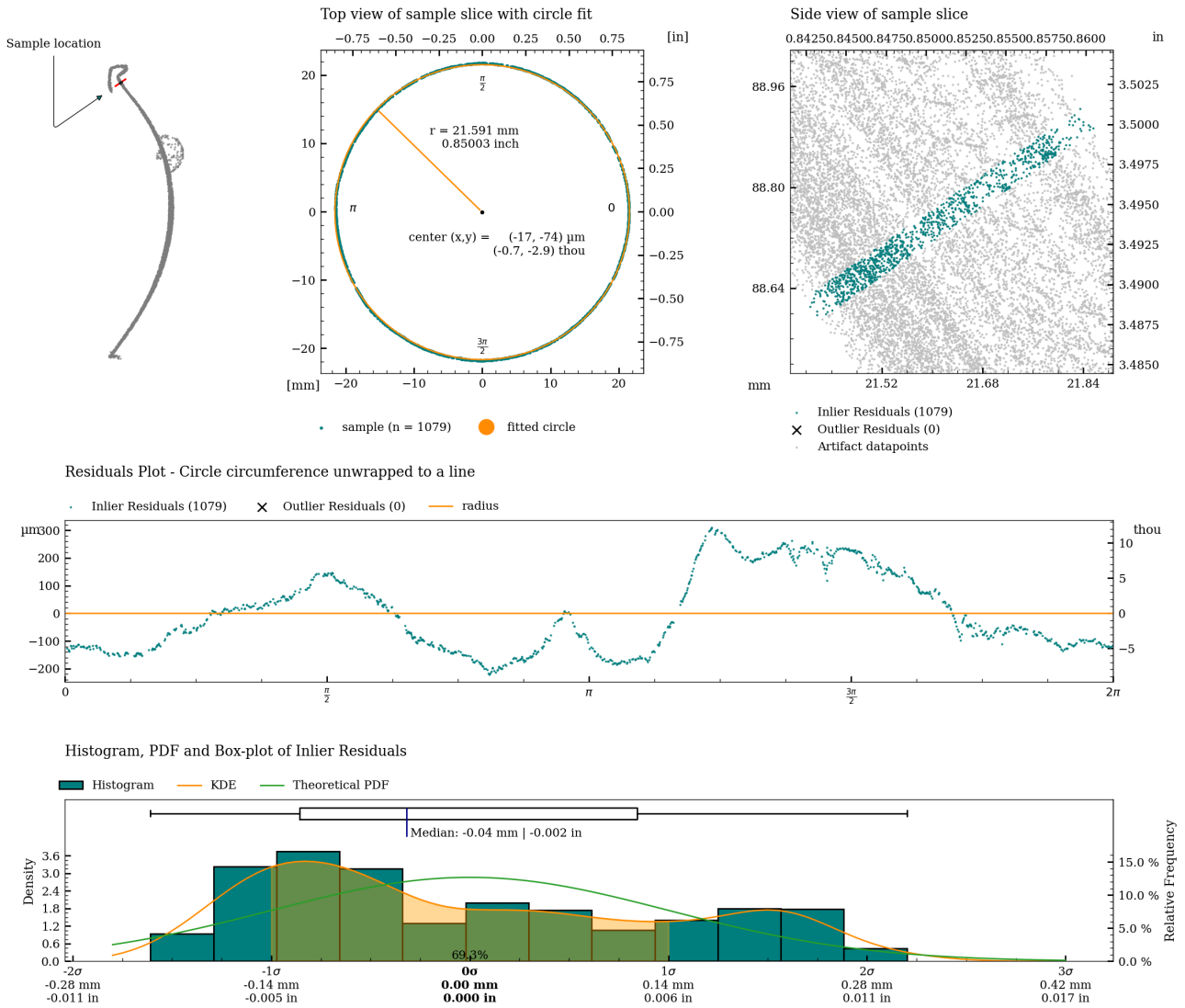

Figure 23: Detailed plot of concentricity measurement for c01.

Copyright 2025, Stine Gerdes - This work is licensed under CC BY-NC-SA 4.0

Concentricity analysis of c02

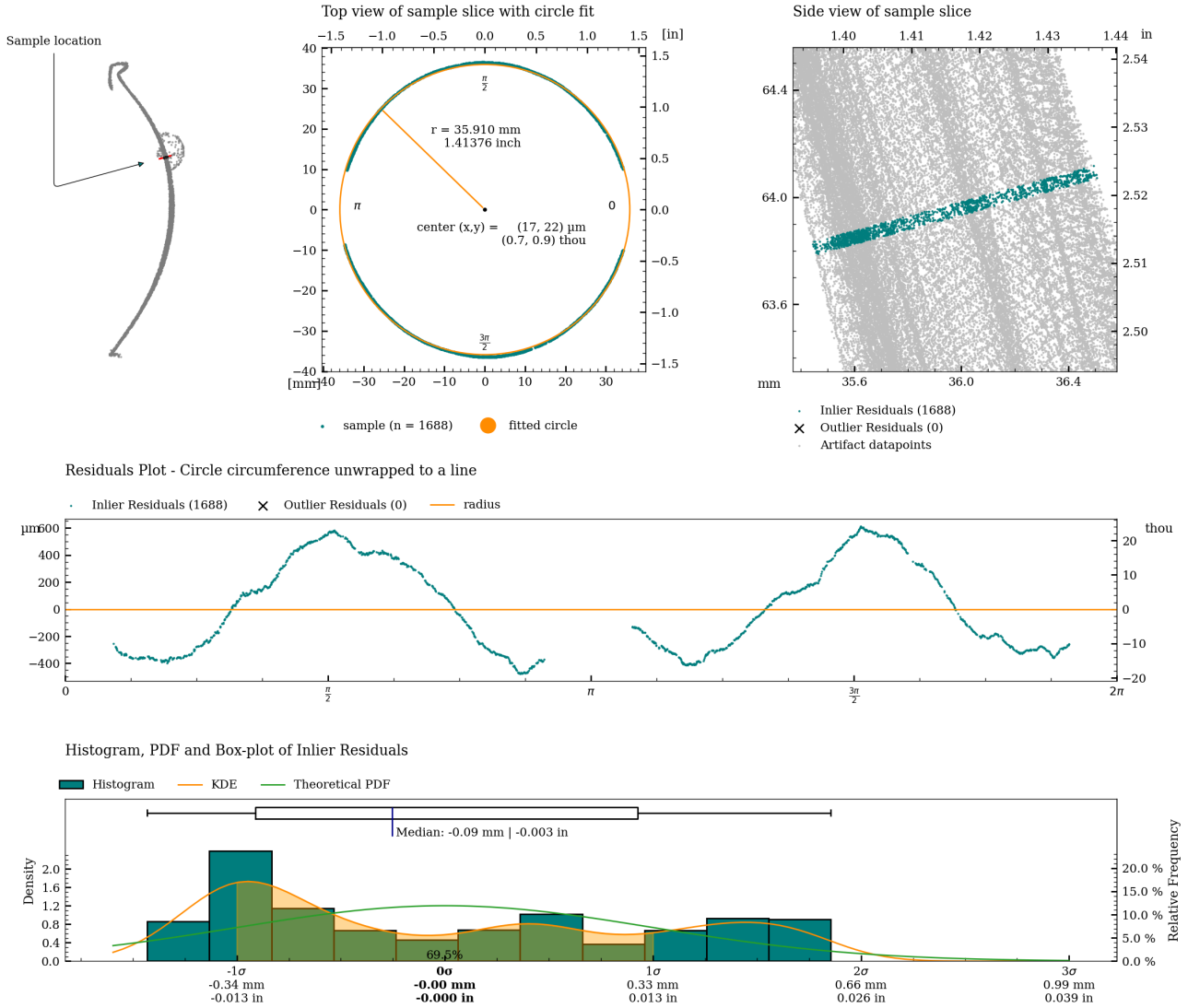

Figure 24: Detailed plot of concentricity measurement for c02.

Copyright 2025, Stine Gerdes - This work is licensed under CC BY-NC-SA 4.0

Concentricity analysis of c03

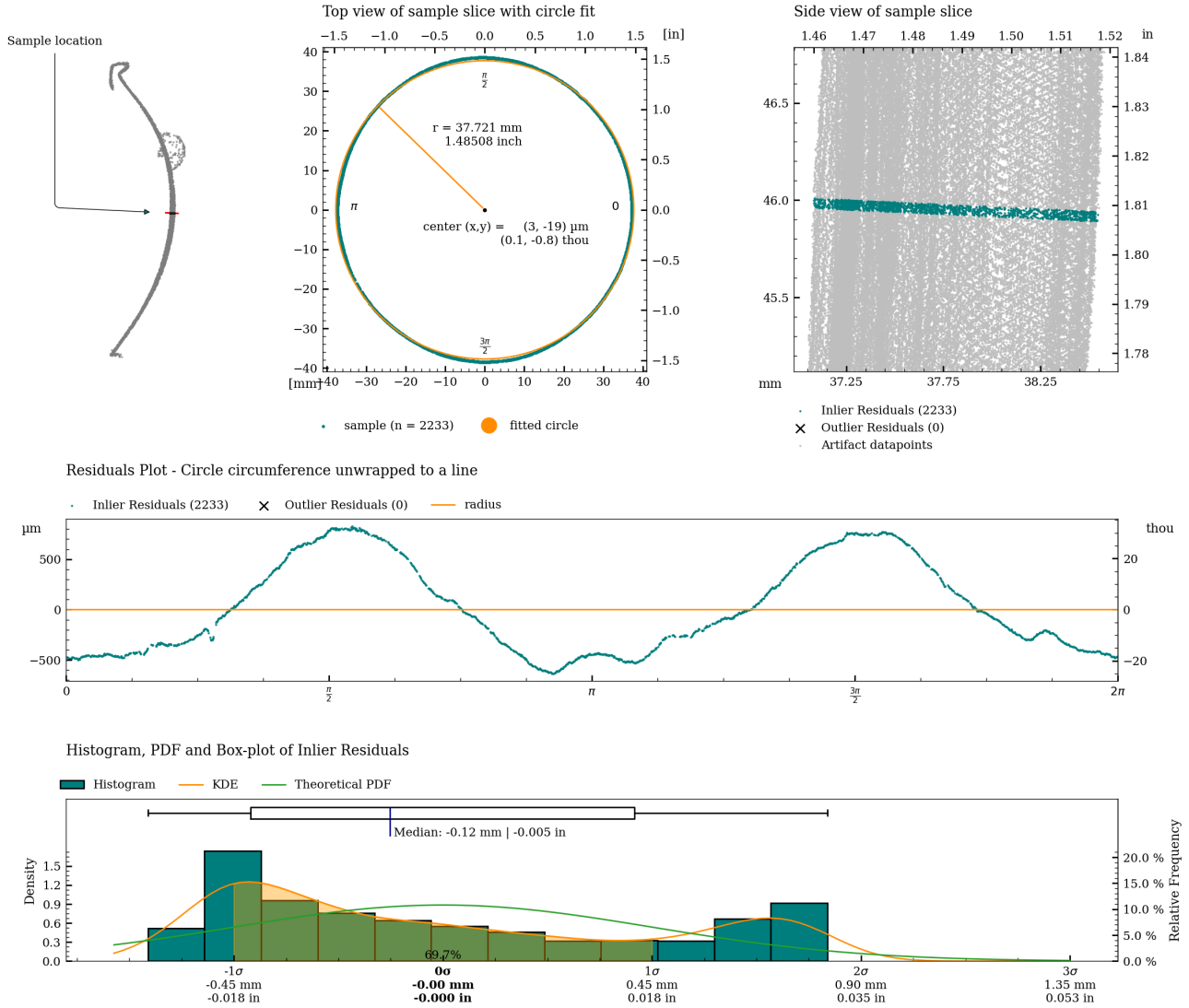

Figure 25: Detailed plot of concentricity measurement for c03.

Copyright 2025, Stine Gerdes - This work is licensed under CC BY-NC-SA 4.0

Concentricity analysis of c04

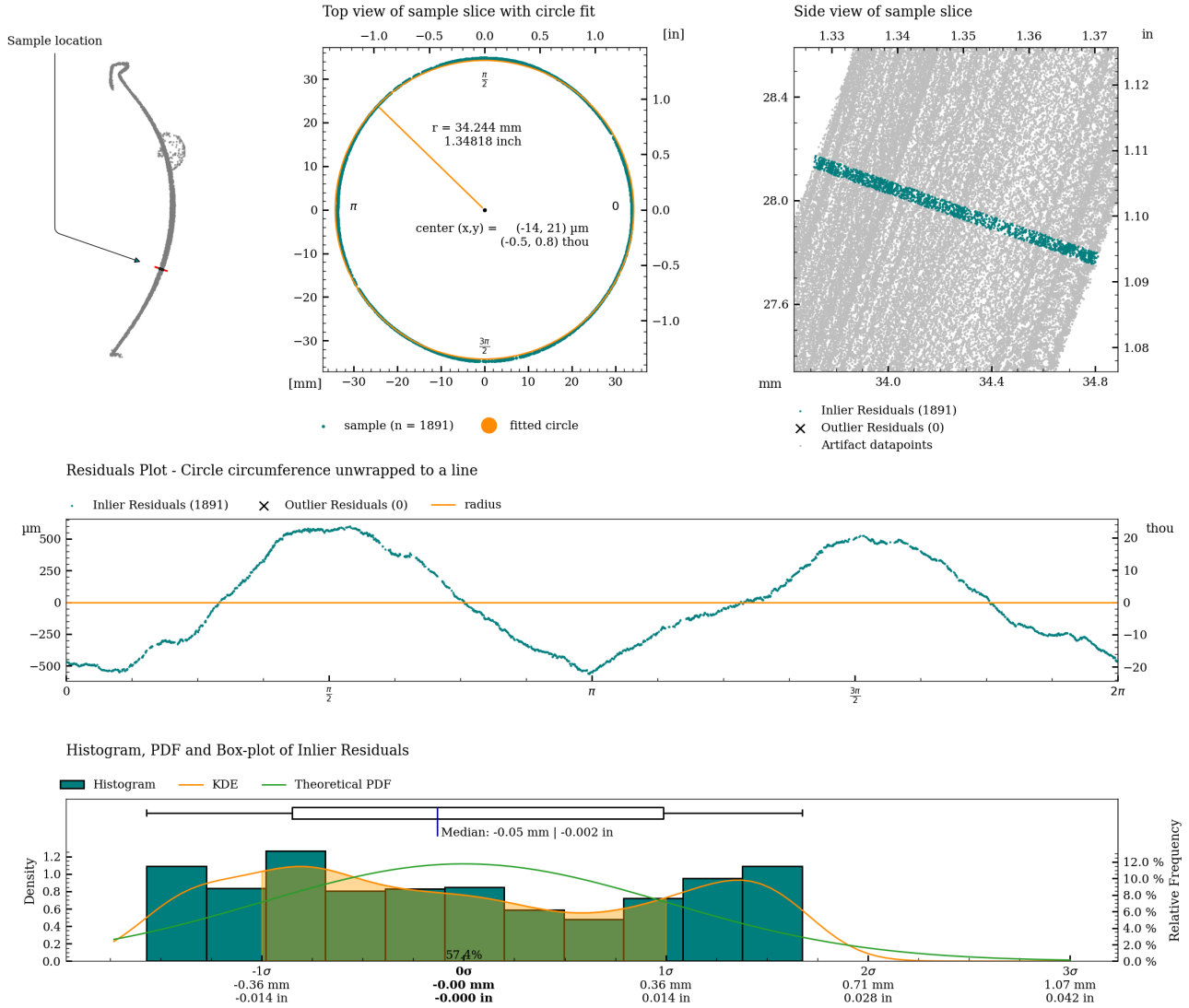

Figure 26: Detailed plot of concentricity measurement for c04.

Copyright 2025, Stine Gerdes - This work is licensed under CC BY-NC-SA 4.0

Concentricity analysis of c05

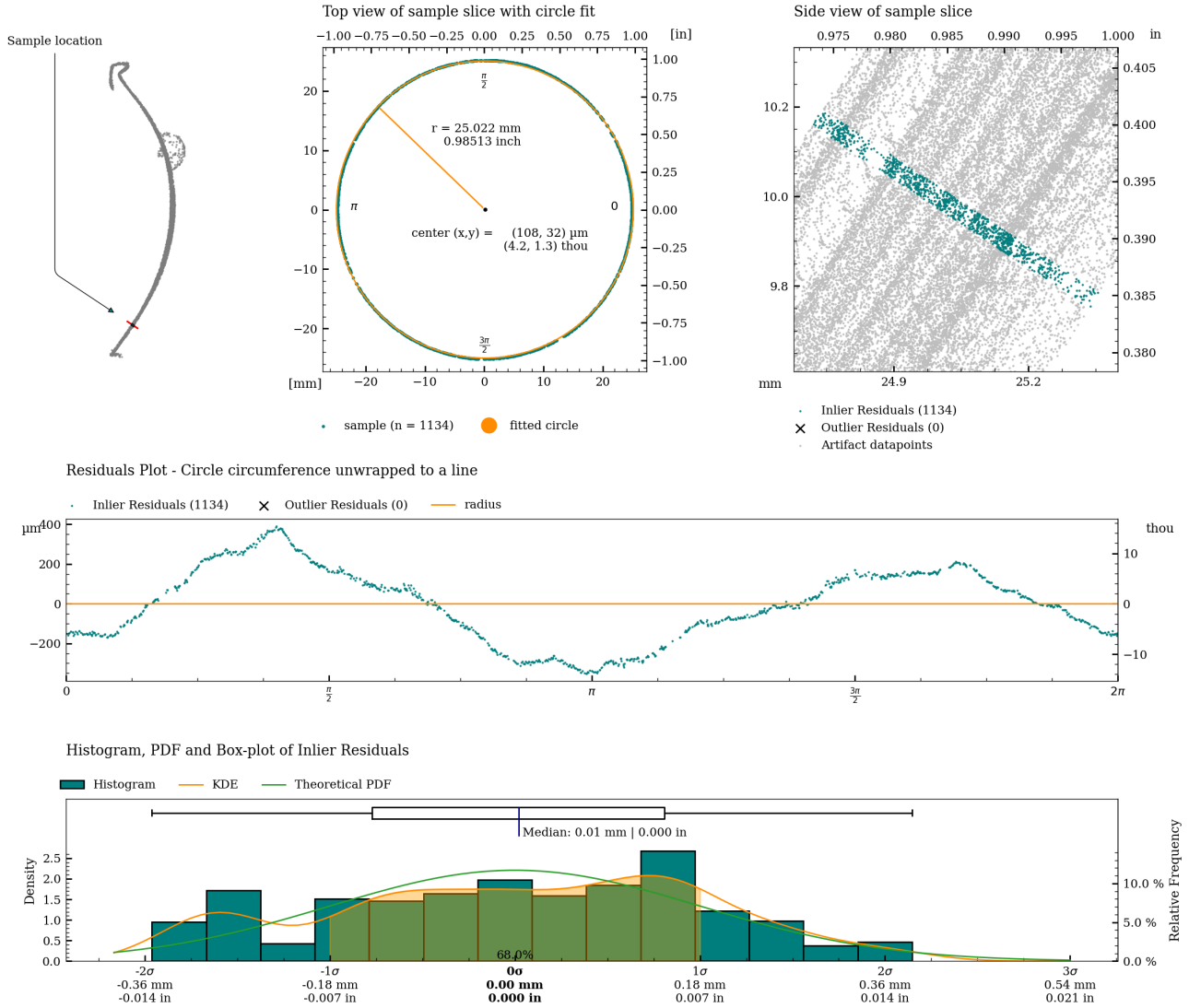

Figure 27: Detailed plot of concentricity measurement for c05.

Copyright 2025, Stine Gerdes - This work is licensed under CC BY-NC-SA 4.0

Concentricity analysis of c06

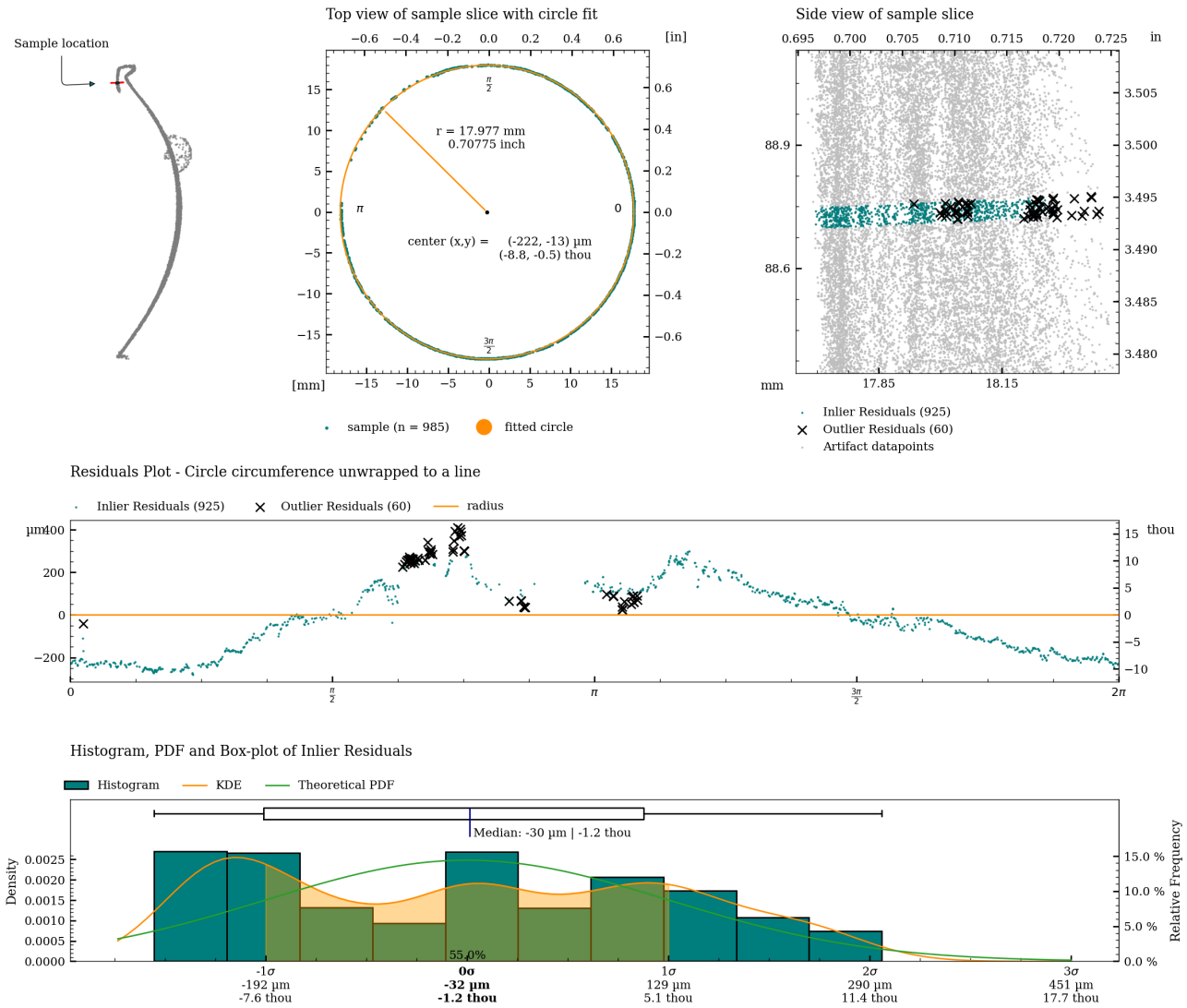

Figure 28: Detailed plot of concentricity measurement for c06.

Copyright 2025, Stine Gerdes - This work is licensed under CC BY-NC-SA 4.0

Coaxiality

Coaxiality is a measure of the deviation in the central axis of an object. Coaxiality measurements are calculated using RANSAC (Random sample consensus) algorithm for outlier detection of a least squares circle regression on cross-sections of the vessel (excluding potential handles) to estimate the best fit circle centers for each slice of the vessel.

Coaxiality is measured for:

- The exterior surface (excluding handles)
- The interior surface

	Exterior		Interior	
Analyzed Slices		1800		165
Median sample size		1630		1019
Slice Height	50 µm	2.0 thou	50 µm	2.0 thou
Statistics with Z-axis as Reference				
Median Absolute Deviation (MAD)	26 µm	1.0 thou	200 µm	7.9 thou
Standard Deviation (SD)	47 µm	1.8 thou	101 µm	4.0 thou
Root Mean Square Deviation (RMSD)	65 µm	2.6 thou	257 µm	10.1 thou
Statistics with Best Fit Central Axis as Reference				
Best fit Central Axis Equation (in metric coordinate system with unit [mm])	x = 0.078 + t-0.00125 y = 0.007 + t-0.00024 z = 0.000 + t1.00000		x = -3.699 + t0.03896 y = 4.511 + t-0.05021 z = 0.000 + t0.99798	
Axis tilt		−0.072°		2.341°
Median Absolute Deviation (MAD)	33 µm	1.3 thou	64 µm	2.5 thou
Standard Deviation (SD)	31 µm	1.2 thou	34 µm	1.3 thou
Root Mean Square Deviation (RMSD)	51 µm	2.0 thou	76 µm	3.0 thou

Table 4: Coaxiality analysis of vessel MV021.

Copyright 2025, Stine Gerdes - This work is licensed under CC BY-NC-SA 4.0

Coaxiality plots, exterior surface

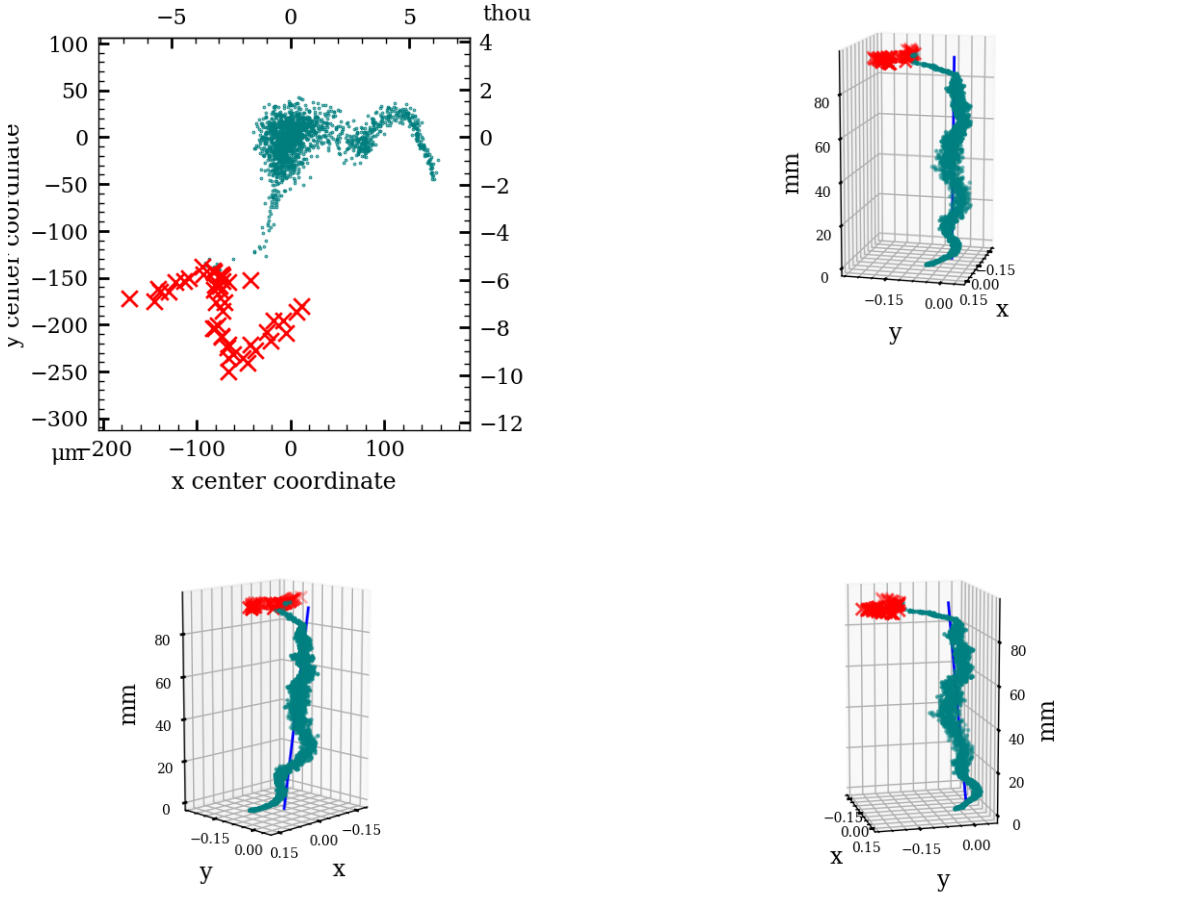

Coaxiality residuals from fitted axis, exterior surface

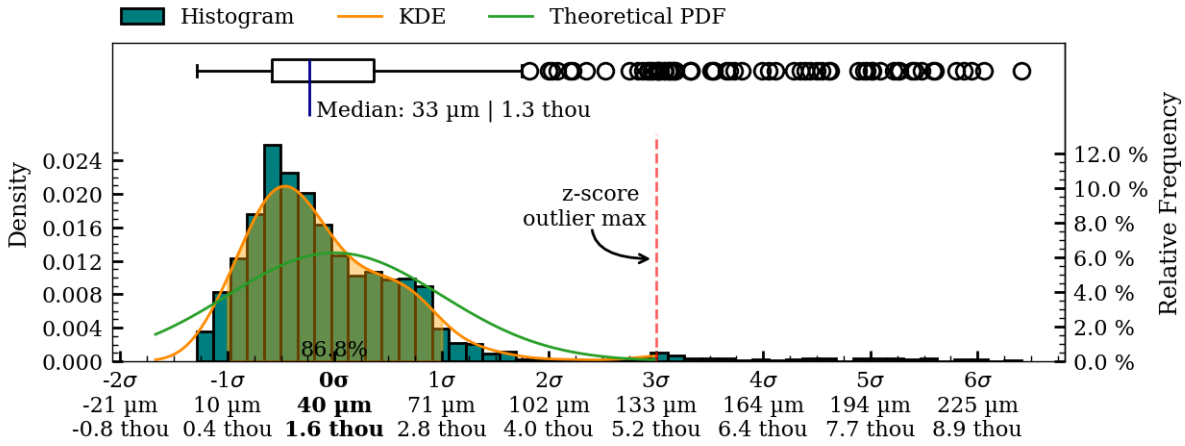

Figure 29: Coaxiality residual plots of exterior surface, MV021.

Copyright 2025, Stine Gerdes - This work is licensed under CC BY-NC-SA 4.0

Coaxiality plots, interior surface

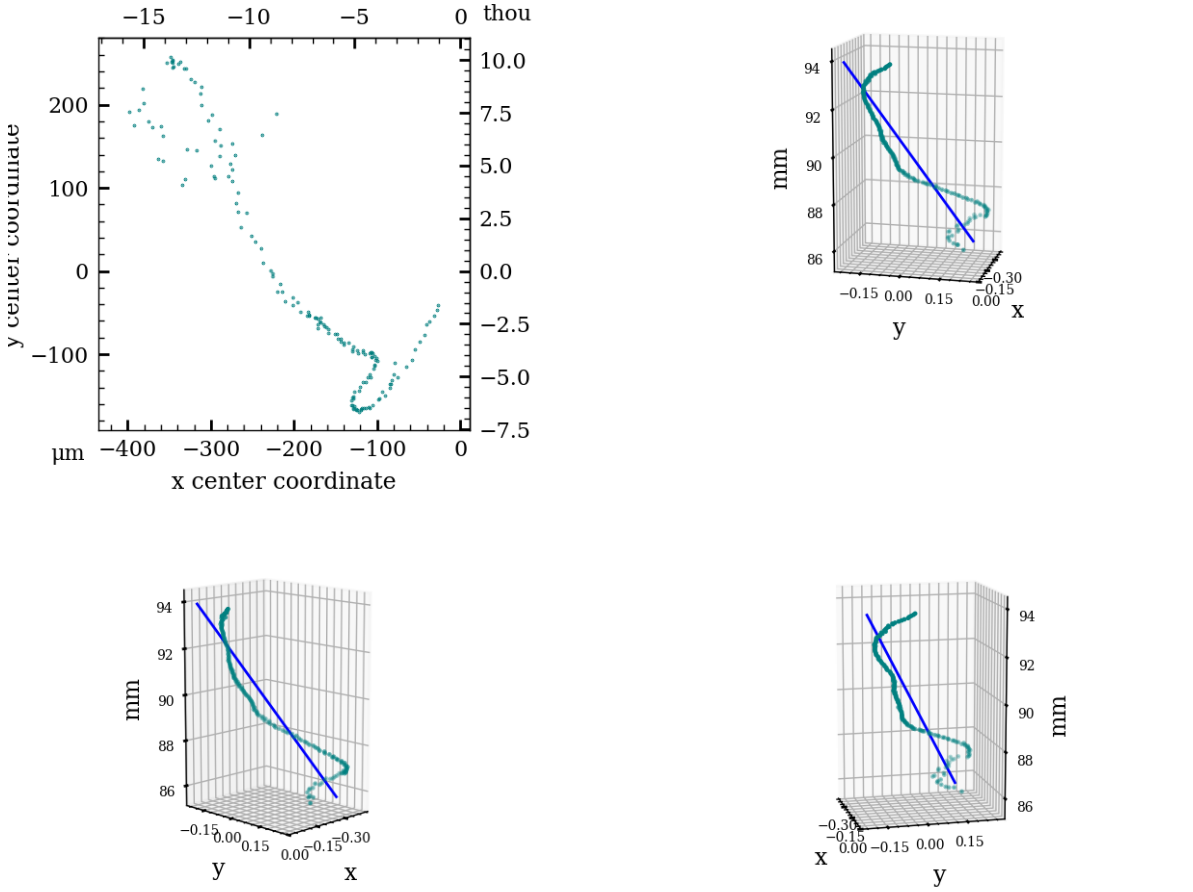

Coaxiality residuals from fitted axis, interior surface

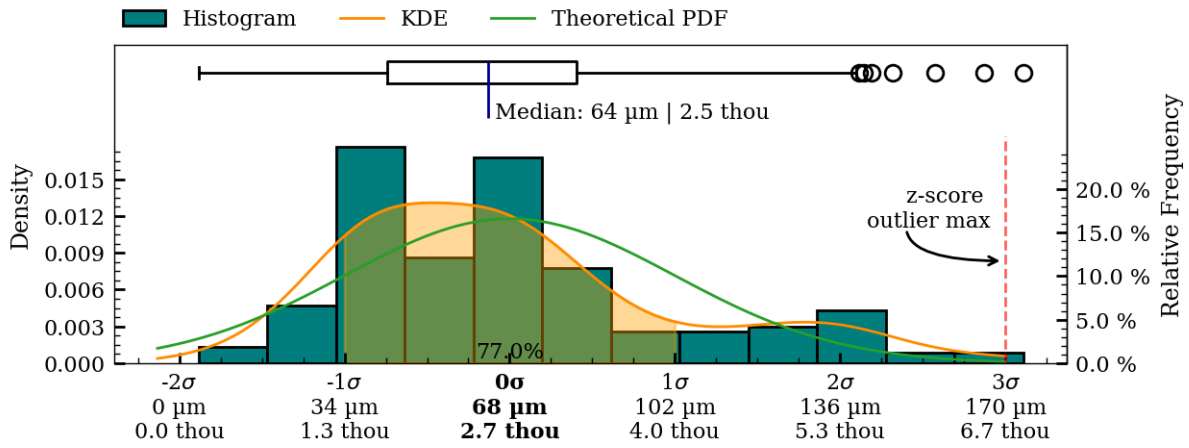

Figure 30: Coaxiality residual plots of interior surface, MV021.

Copyright 2025, Stine Gerdes - This work is licensed under CC BY-NC-SA 4.0

Surface Variability

To illustrate the overall surface deviations of the object, a surface variability heatmap has been created. This heatmap provides an accessible overview of the topography of the manufacturing precision and surface structure of the object.

The surface variability measurements are created by fitting a number of higher-order polynomials to the two-dimensional folded profile of the scan data. This process creates an idealized mathematical representation of actual surface curvature of object, and as such provides a continuous model representation of the actual object. It is important to note that only such a non-discretized representation is sufficient to avoid introducing inconsistently varying errors in the mapping of the final surface deviation results, that the rendered heatmaps are based on.

To produce the final surface variability map, the distance from each scanned vertex to the fitted polynomial is calculated and used as the mapping function input, for applying colours to the surface of the object.

It is important to note that this variability map does not describe deviations from the original *intended* shape of the artifact (if any), as this shape (the *intended design*, so to speak) will have been lost to time. It does however provide a very informative visualization of the texture and structure of the surface and very importantly, *does* hightlight potential manufacturing-relevant patterns in the surface texture (if present). Such patterns are, as an example, clearly evident on the interior surface of artifact PV001.

Copyright 2025, Stine Gerdes - This work is licensed under CC BY-NC-SA 4.0

Exterior surface

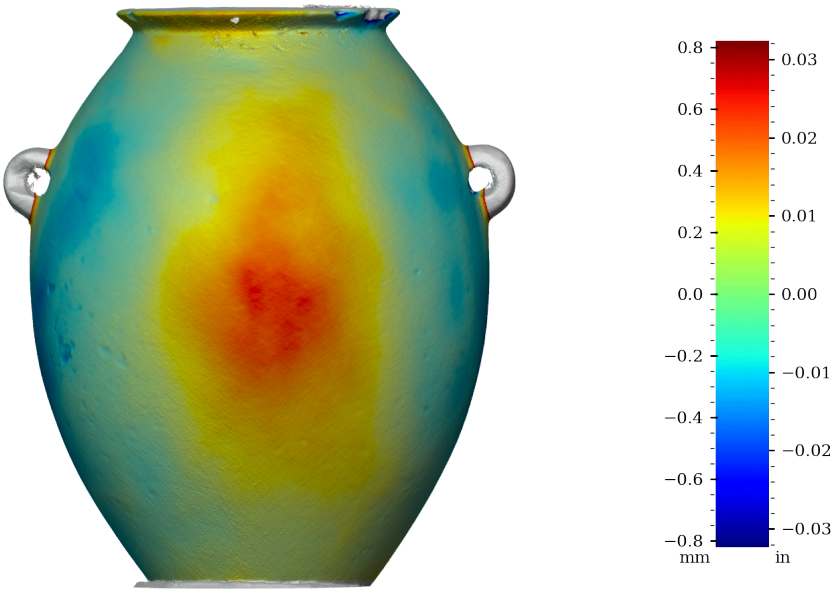

Figure 31: Surface variability heatmap of MV021, front view

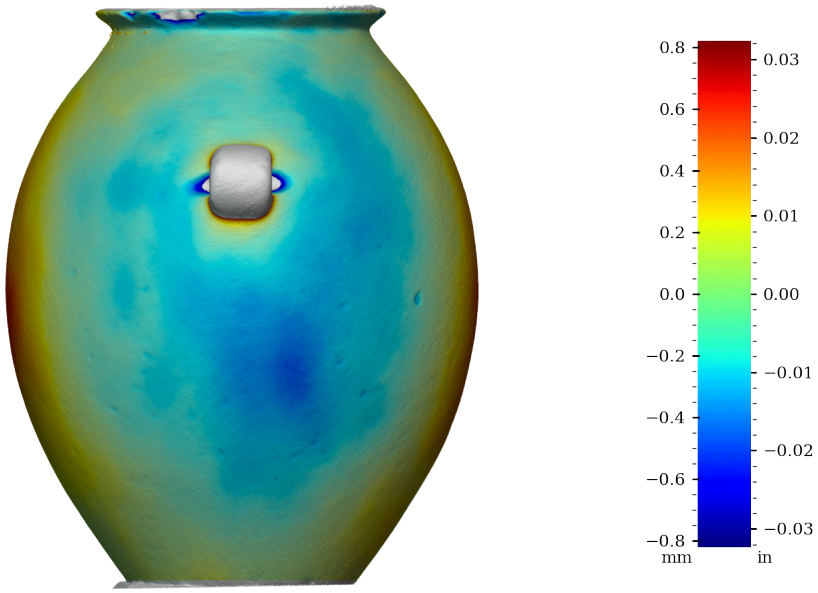

Figure 32: Surface variability heatmap of MV021, rotated 90°

Copyright 2025, Stine Gerdes - This work is licensed under CC BY-NC-SA 4.0

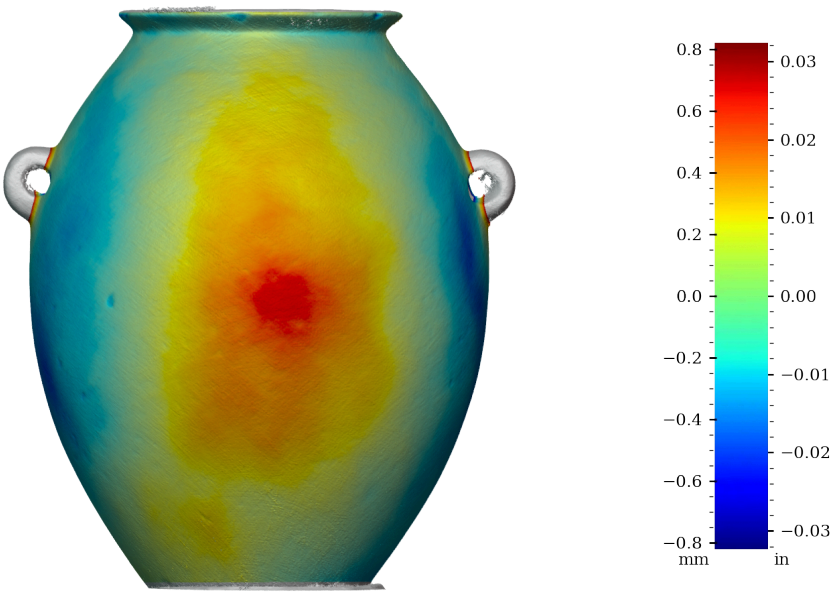

Figure 33: Surface variability heatmap of MV021, rotated 180°

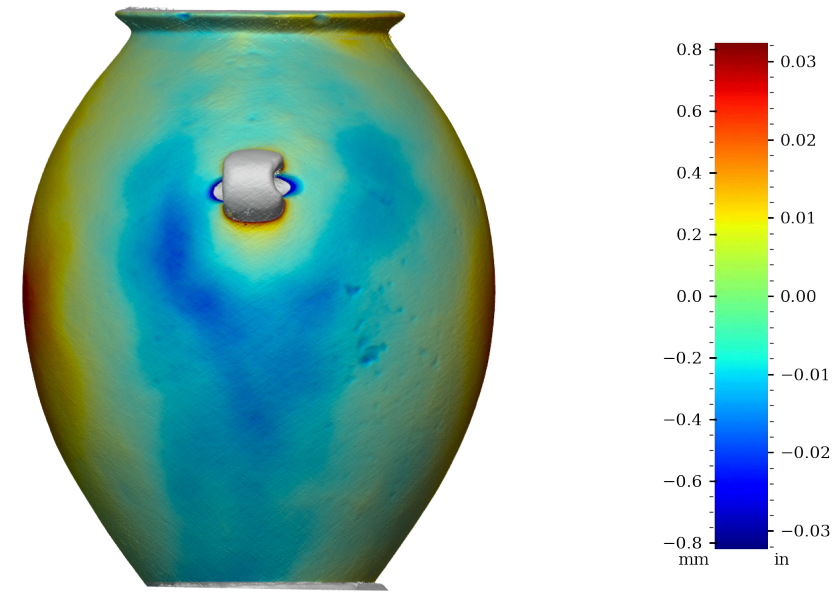

Figure 34: Surface variability heatmap of MV021, rotated 270°

Copyright 2025, Stine Gerdes - This work is licensed under CC BY-NC-SA 4.0

Interior surface

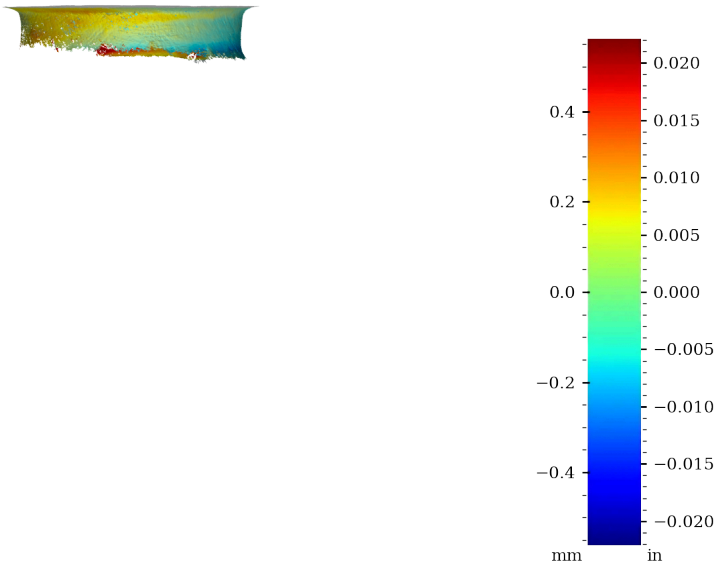

Figure 35: Surface variability heatmap of MV021, front view

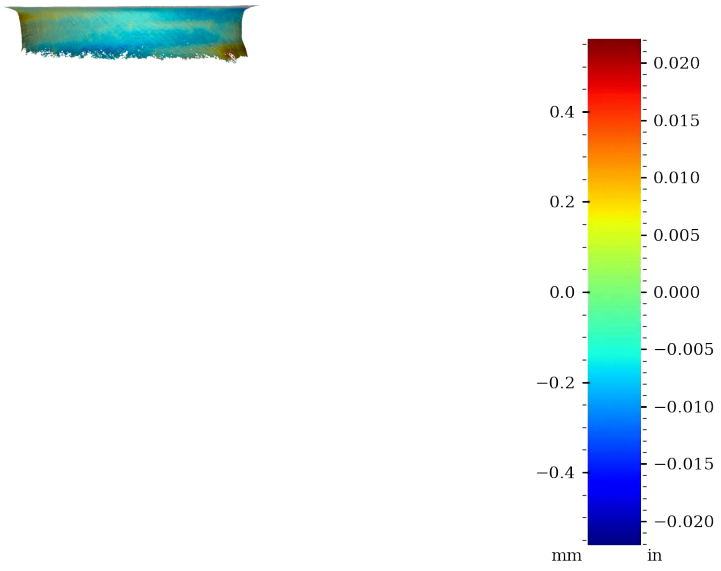

Figure 36: Surface variability heatmap of MV021, rotated 90°

Copyright 2025, Stine Gerdes - This work is licensed under CC BY-NC-SA 4.0

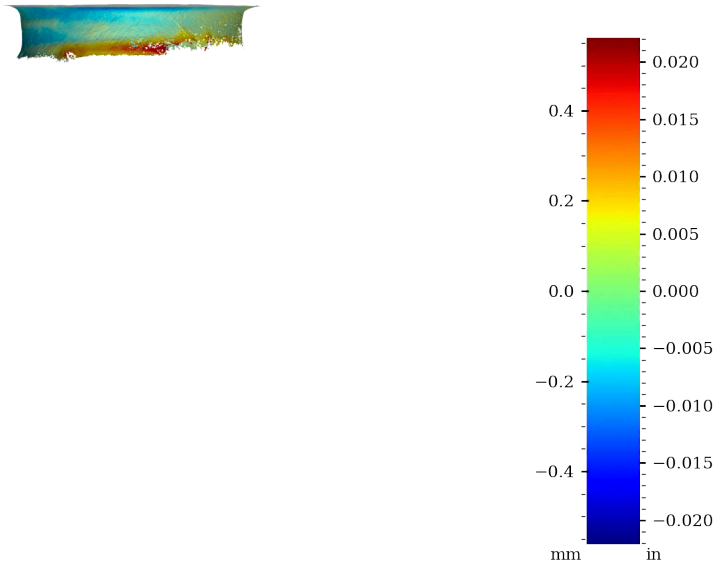

Figure 37: Surface variability heatmap of MV021, rotated 180°

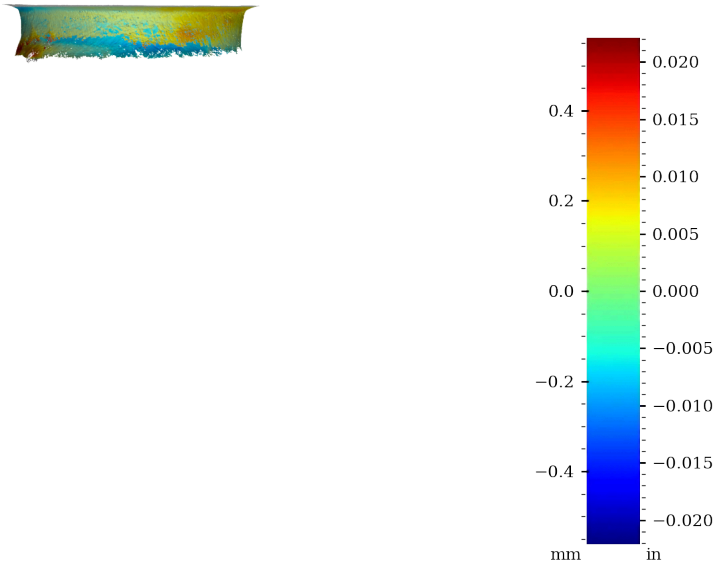

Figure 38: Surface variability heatmap of MV021, rotated 270°

Copyright 2025, Stine Gerdes - This work is licensed under CC BY-NC-SA 4.0

Surface variability statistics

Area	MSD	RMSD	SD	Mean AD	Median AD	Range	Min	Max	Sample size
	mm^2	mm	mm	mm	mm	mm	mm	mm	
Exterior	0.1034	0.322	0.322	0.240	0.269	1.486	−0.666	0.820	3508139
Interior	0.0301	0.174	0.173	0.134	0.144	1.624	−0.900	0.725	186315
	in^2	in	in	in	in	in	in	in	
Exterior	0.000160	0.0127	0.0127	0.0094	0.0106	0.0585	−0.0262	0.0323	3508139
Interior	0.000047	0.0068	0.0068	0.0053	0.0057	0.0639	−0.0354	0.0285	186315

Table 5: Surface variability statistics, MV021

Table 5 shows the statistics of the distance from the scan vertices to the best fit object model. These statistics are briefly explained below.

Mean Squared Deviation (MSD), also known as Mean Squared Error (MSE).

$$\mathrm{MSD} = \frac{\sum_{i=1}^{n} (y_i - \hat{y})^2}{n}$$

The MSD metric shows the the average squared difference between the scanned points and the fitted composite polynomial model (a value of 0 would be a perfect match). This metric emphasizes imperfections in the surface of the artifact. Outliers will negatively influence this metric, raising the value of the MSE.

Root Mean Squared Deviation (RMSD), also known as Root Mean Squared Error (RMSE).

$$\mathrm{RMSD} = \sqrt{\frac{\sum_{i=1}^{n} (y_i - \hat{y})^2}{n}}$$

Measures the dispersion of the measured surface variability y_i around a model predictor ($\hat{y}$). By obtaining the root of the MSD, the exponent will be removed from the measurement, enabling comparisons with other statistics of the same unit and making it more accessible to those familiar with the RMSD metric. This measure is used to assess the fit of a regression model to a dataset, in this case our best fit composite polynomial model. The lower the RMSD metric, the better the fit.

Standard Deviation (SD)

$$s = \sqrt{\frac{\sum_{i=1}^{n} (y_i - \bar{y})^2}{n-1}}$$

Measures the dispersion of the measured surface variability y_i around the mean ($\bar{y}$). If the residuals are normally distributed around the mean ($\bar{y} \approx 0$), the SD will be equal to the RMSD. See Figure 39 and Figure 40

Mean Absolute Deviation (MeanAD)

$$\mathrm{MeanAD} = \frac{\sum_{i=1}^{n} |y_i - \bar{y}|}{n}$$

This metric is similar to the SD, but the difference between the residuals and the mean is *not* squared. Instead of indicating the spread of the data, we look at the average distance between each data point and the mean. The Mean Absolute Deviation is affected less by outliers than the Standard Deviation.

Median Absolute Deviation (MedianAD)

$$\mathrm{MedianAD} = \mathrm{median}(|y_i - \mathrm{median}(y)|)$$

The Median Absolute Deviation is measure of the dispersion of the data around the median.

Range

$$\max(y_i) - \min(y_i)$$

Range is a measure of the total spread of the residuals

Copyright 2025, Stine Gerdes - This work is licensed under CC BY-NC-SA 4.0

Histogram, KDE and Box-plot of measured surface variability - exterior surface

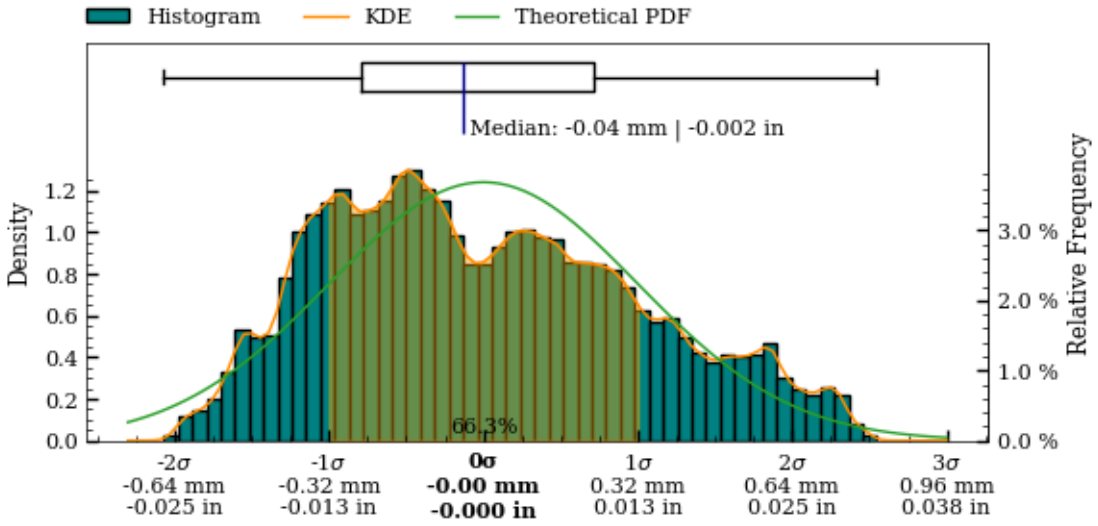

Figure 39: Exterior surface variability boxplot, kds and histogram.

Histogram, KDE and Box-plot of measured surface variability - interior surface

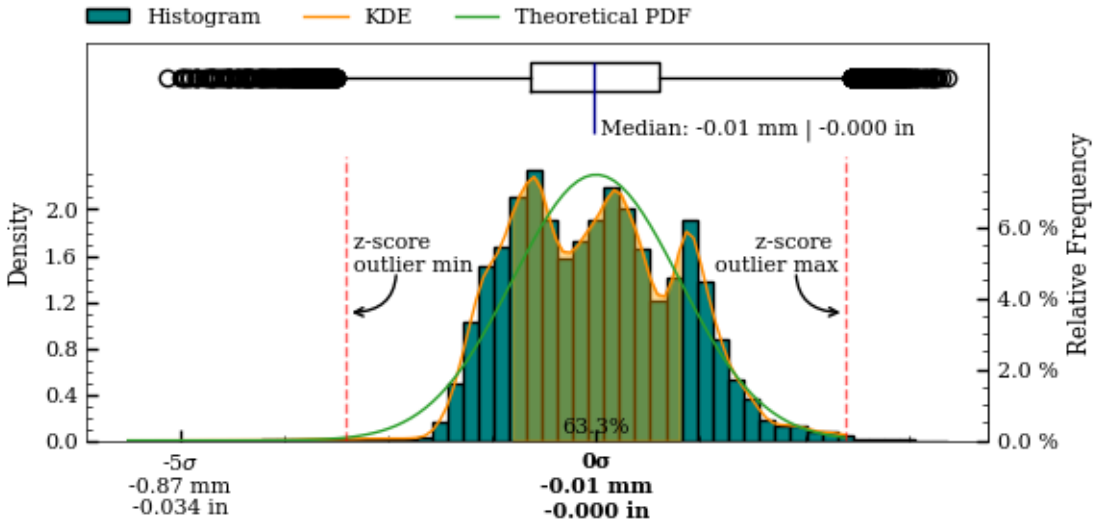

Figure 40: Interior surface variability boxplot, kds and histogram.

Copyright 2025, Stine Gerdes - This work is licensed under CC BY-NC-SA 4.0

Precision Score Of The Artifact

To enable valid comparison of the manufacturing precision of different artifacts, a metric that robustly quantifies the overall precision of the object is required. The considerations for such a metric will be explored in this section.

Based on these considerations, a *Precision Score* metric will be defined.

For an object to be described as having been manufactured with high precision, several qualities must be present *concurrently*, and throughout the *entire* geometry of the final object. A given object may exhibit high levels of one or more *components* of precision, but be lacking in others. For example:

- An object may present high levels of coaxialility, but lack circularity.
- An object may exhibit good circularity, but show imperfections in the surface structure.
- An object may be smoothed to perfection *without* any circularity or coaxiality.
- An object may exhibit high levels of all of the above metrics in *some* areas, but not in others.

Therefore, a precision score metric **must** account for *all* aspects of the individual, underlying precision metrics (circularity, concentricity, coaxiality and surface variability) throughout the *entire* surface area of the object.

The composite high order polynomial model, used to generate the surface variability map (described in Surface Variability, p. 33) is the best continuous mathematical representation of the object available to us (lacking any original design plans, as would normally be available in metrological analysis). This idealized model encompasses all of the above component metrics.

In the creation of the model, all scan data-points are taken into account (excluding areas with extensive damage), making it the best possible idealized representation we can achieve. When this model has been accurately created, the deviation between the model and the scanned data-points can be calculated over the non-discretized polynomials, *without* the need for an "original" CAD model (and importantly, unless such a CAD model *actually* corresponded to the original design intent, it would be an insufficient comparison basis).

Within the context of defining a valid, overall precision metric, this approach satisfies the incorporation of all of the necessary metrics:

- **Circularity**: Because the reconstructed polynomial model is revolved around the Z-plane, the idealized representation is perfectly circular, and thus incorporates the circularity component.
- **Concentricity and coaxiality**: Because the Z-axis (datum axis) is the center axis of the model, it incorporates the concentricity and coaxiality components.
- **Surface variability**: Because the model is continuous and non-discretized, it can be used accurately for all points of the scan data, and incorporates the surface variability component.

The level of precision ultimately achieved in a physical object does not share a linear relationship with its manufacturing requirements. Since continuously higher levels of final precision becomes progressively harder to achieve, an overall precision metric must take this relationship into account.

A robust statistical metric that satisfies this requirement is the *Mean Squared Deviation* (MSD or MSE). Here specifically, we can utilize the mean square of the deviations between the model ($\hat{y}$) and the data-points (y_i).

Combining all of the above considerations, we can express a well-defined *Precision Score* metric, that provides an immediately accessible way to understand the overall precision of an object, while being statistically valid. Since the Mean Squared Deviation tends towards zero as the overall precision increases, the inverse of the Mean Squared Deviation is taken to obtain a precision score metric that increases as precision increases[12]:

$$\text{Precision Score} = \frac{n}{\sum_{i=1}^{n} (y_i - \hat{y})^2}$$

[12] The precision score unit is $\frac{1}{\text{mm}^2}$

Copyright 2025, Stine Gerdes - This work is licensed under CC BY-NC-SA 4.0

A precision score will be calculated seperately for:

- The exterior surface
- The interior surface
- The full surface

As most scans do not include sufficient scan data for the interior surface, the exterior surface will be used for calculating the precision score in most cases. In the rare case that the scan data is more complete for the *interior* surface, this will be used instead.

Table 6 shows the precision score of this artifact (MV021), compared to the two most precise, and the two least precise vessels currently analyzed.

Artifact			Material	Precision Score	Link to Report
	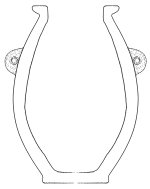	PV001	Red Granite	**1905** Full: 980 Exterior: 1905 Interior: 705	Report Publication
	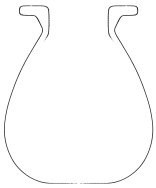	PV006	Dark grey granite	**621** Full: 521 Exterior: 621 Interior: 152	Report Publication
	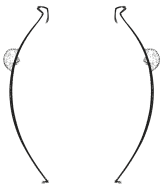	MV021	Grey Basalt	**10** Full: 10 Exterior: 10 Interior: 33	Report Publication
	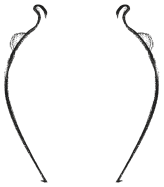	MV001	Pottery	**1.93** Full: 1.92 Exterior: 1.93 Interior: 1.85	Report Publication
	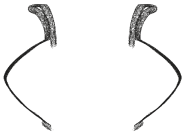	MV010	Calcite (Egyptian Alabaster)	**1.12** Full: 0.64 Exterior: 1.12 Interior: 0.20	Report Publication

Copyright 2025, Stine Gerdes - This work is licensed under CC BY-NC-SA 4.0

Analysis Roadmap

While the current iteration of this work already provides valuable results, continued future additions and improvements will enhance their utility further. This section details planned iterative updates and improvements, to both the reports themselves, and to the underlying methodology and software they are created with.

Alignment Section

- Detailed exploration of different circle regression algorithms
- If handles are present on the vessel, exploring alignment of the vessels so the handle positions match each other
- Add optimization of the perpendicular surface deviation, with the best results of the coaxial alignment
- Align by minimizing circularity results (of rotated sample slice, to compensate for sample height distortions)

Measurements of Precision

- Section detailing how measurements perpendicular to the surface curvature are obtained
- Detailed surface area analysis, exploring the residual patterns throughout subsequent sample slices of the artifact surface
- Wall thickness deviation color map
- Robust outlier identification on circularity, to better handle analysis of damaged areas of the artifacts in addition to removal of interior crystalline structure points present in CT scans
- Layout updates to the charts and tables

Visibility of Outliers and Damaged Sections

- Identification and marking of damaged parts
- Visualization of outliers on the artifact surface

Exploration of Mathematical Primitives

- Analysis of selected curvatures and flat surfaces on the vessel in both the horizontal and vertical planes
  - Circles
  - Parabolas
  - Ellipsoids
  - Hyperbolas
  - Cones
- Implementation of robust regressions models suitable for this domain, based on RANSAC.

Metrics on Primary Features

- Measurements of features in the horizontal plane
- Measurements of features in the vertical plane
- Measurements of angles
- Measurements of volume

Exploration of Potential Design Ratios

- π, φ, e, 1, 2, 3, 4 etc.

Raw Dataset Attachments

- Including all measurement and sample coordinates as CSV-files embedded in the report
- Including an STL file of the aligned object alongside the report, for easier external replication and validation of the research results

Copyright 2025, Stine Gerdes - This work is licensed under CC BY-NC-SA 4.0

Appendix A - Comparison Of Circularity Measurements (Z-plane vs. surface-perpendicular)

Comparison of circularity samples

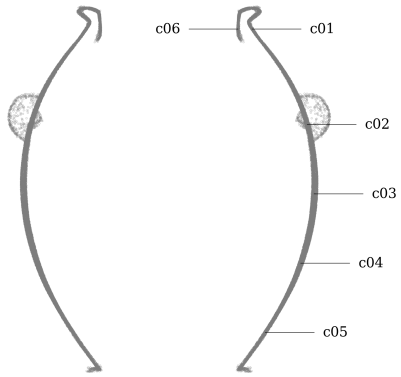

Samples perpendicular to the surface curvature

Tag	Area	Measured deviation[8]	Residuals				Sample size	Slice		
			Range	RMSD[9]	MAD[10]	SD		Height	Z coord.	Radius[11]
		mm	mm	mm	mm	mm		mm	mm	mm
c01	exterior	Ø43.185±0.307	0.531	0.139	0.119	0.139	1079	0.050	88.734	21.593
c02	exterior	Ø71.861±0.591	1.089	0.332	0.320	0.332	1682	0.050	63.941	35.931
c03	exterior	Ø75.456±0.819	1.464	0.451	0.421	0.451	2236	0.050	45.954	37.728
c04	exterior	Ø68.488±0.596	1.159	0.358	0.323	0.358	1889	0.050	27.968	34.244
c05	exterior	Ø50.051±0.387	0.742	0.181	0.143	0.181	1134	0.050	9.981	25.026
c06	interior	Ø35.924±0.424	0.690	0.169	0.151	0.169	985	0.050	88.734	17.962

Table 7: Detailed circularity measurements at selected samples in z-plane, vessel MV021.

Samples in the Z-plane

Tag	Area	Measured deviation[8]	Residuals				Sample size	Slice		
			Range	RMSD[9]	MAD[10]	SD		Height	Z coord.	Radius[11]
		mm	mm	mm	mm	mm		mm	mm	mm
c01	exterior	Ø43.107±0.476	0.724	0.177	0.130	0.172	1496	0.050	88.734	21.553
c02	exterior	Ø71.703±0.693	1.130	0.345	0.277	0.339	1749	0.050	63.941	35.852
c03	exterior	Ø75.258±0.920	1.469	0.469	0.354	0.457	2260	0.050	45.954	37.629
c04	exterior	Ø68.373±0.697	1.238	0.383	0.328	0.379	2186	0.050	27.968	34.186
c05	exterior	Ø50.071±0.466	0.916	0.220	0.167	0.219	1739	0.050	9.981	25.035
c06	interior	Ø35.916±0.429	0.691	0.168	0.150	0.168	977	0.050	88.734	17.958

Table 8: Detailed circularity measurements at selected samples perpendicular to vessel curvature, vessel MV021.

Copyright 2025, Stine Gerdes - This work is licensed under CC BY-NC-SA 4.0

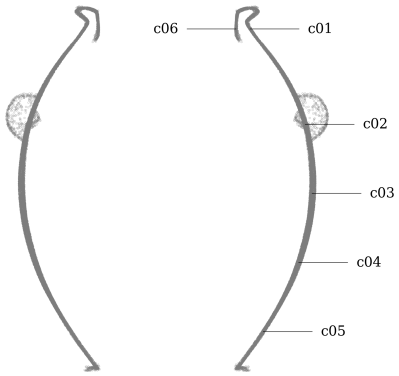

Samples perpendicular to the surface curvature

Tag	Area	Measured deviation[8]	Residuals				Sample size	Slice		
			Range	RMSD[9]	MAD[10]	SD		Height	Z coord.	Radius[11]
		in	in	in	in	in		in	in	in
c01	exterior	Ø1.7002±0.0121	0.0209	0.0055	0.0047	0.0055	1079	0.0020	3.4935	0.8501
c02	exterior	Ø2.8292±0.0233	0.0429	0.0131	0.0126	0.0131	1682	0.0020	2.5173	1.4146
c03	exterior	Ø2.9707±0.0322	0.0576	0.0177	0.0166	0.0177	2236	0.0020	1.8092	1.4854
c04	exterior	Ø2.6964±0.0235	0.0456	0.0141	0.0127	0.0141	1889	0.0020	1.1011	1.3482
c05	exterior	Ø1.9705±0.0152	0.0292	0.0071	0.0056	0.0071	1134	0.0020	0.3930	0.9853
c06	interior	Ø1.4143±0.0167	0.0272	0.0066	0.0059	0.0066	985	0.0020	3.4935	0.7072

Table 9: Detailed circularity measurements at selected samples in z-plane, vessel MV021.

Samples in the Z-plane

Tag	Area	Measured deviation[8]	Residuals				Sample size	Slice		
			Range	RMSD[9]	MAD[10]	SD		Height	Z coord.	Radius[11]
		in	in	in	in	in		in	in	in
c01	exterior	Ø1.6971±0.0188	0.0285	0.0070	0.0051	0.0068	1496	0.0020	3.4935	0.8486
c02	exterior	Ø2.8230±0.0273	0.0445	0.0136	0.0109	0.0134	1749	0.0020	2.5173	1.4115
c03	exterior	Ø2.9629±0.0362	0.0578	0.0185	0.0139	0.0180	2260	0.0020	1.8092	1.4815
c04	exterior	Ø2.6918±0.0274	0.0487	0.0151	0.0129	0.0149	2186	0.0020	1.1011	1.3459
c05	exterior	Ø1.9713±0.0184	0.0361	0.0086	0.0066	0.0086	1739	0.0020	0.3930	0.9856
c06	interior	Ø1.4140±0.0169	0.0272	0.0066	0.0059	0.0066	977	0.0020	3.4935	0.7070

Table 10: Detailed circularity measurements at selected samples perpendicular to vessel curvature, vessel MV021.

Copyright 2025, Stine Gerdes - This work is licensed under CC BY-NC-SA 4.0

Comparison of circularity on the full vessel surface

Metric

Samples perpendicular to the surface curvature

Area	Range			Standard Deviation			Medan Absolute Deviation			Slices	Slice height
	Median	Min.	Max.	Median	Min.	Max.	Median	Min.	Max.		
	mm	mm	mm	mm	mm	mm	mm	mm	mm		mm
Exterior	0.977	0.426	1.467	0.299	0.109	0.458	0.074	0.059	0.373	1800	0.050
Interior	0.643	0.430	1.231	0.166	0.115	0.291	0.027	0.073	0.197	165	0.050

Table 11: Detailed circularity measurements at selected samples in z-plane, vessel MV021.

Samples in the z-plane

Area	Range			Standard Deviation			Medan Absolute Deviation			Slices	Slice height
	Median	Min.	Max.	Median	Min.	Max.	Median	Min.	Max.		
	mm	mm	mm	mm	mm	mm	mm	mm	mm		mm
Exterior	1.093	0.549	1.545	0.328	0.139	0.459	0.065	0.080	0.382	1798	0.050
Interior	0.697	0.436	2.225	0.168	0.117	0.607	0.034	0.076	0.572	167	0.050

Table 12: Detailed circularity measurements at selected samples perpendicular to vessel curvature, vessel MV021.

Imperial

Samples perpendicular to the surface curvature

Area	Range			Standard Deviation			Medan Absolute Deviation			Slices	Slice height
	Median	Min.	Max.	Median	Min.	Max.	Median	Min.	Max.		
	in	in	in	in	in	in	in	in	in		in
Exterior	0.977	0.426	1.467	0.299	0.109	0.458	0.074	0.059	0.373	1800	0.050
Interior	0.643	0.430	1.231	0.166	0.115	0.291	0.027	0.073	0.197	165	0.050

Table 13: Detailed circularity measurements at selected samples in z-plane, vessel MV021.

Samples in the z-plane

Area	Range			Standard Deviation			Medan Absolute Deviation			Slices	Slice height
	Median	Min.	Max.	Median	Min.	Max.	Median	Min.	Max.		
	in	in	in	in	in	in	in	in	in		in
Exterior	1.093	0.549	1.545	0.328	0.139	0.459	0.065	0.080	0.382	1798	0.050
Interior	0.697	0.436	2.225	0.168	0.117	0.607	0.034	0.076	0.572	167	0.050

Table 14: Detailed circularity measurements at selected samples perpendicular to vessel curvature, vessel MV021.

Copyright 2025, Stine Gerdes - This work is licensed under CC BY-NC-SA 4.0

Circularity analysis of exterior samples perpendicular to surface curvature

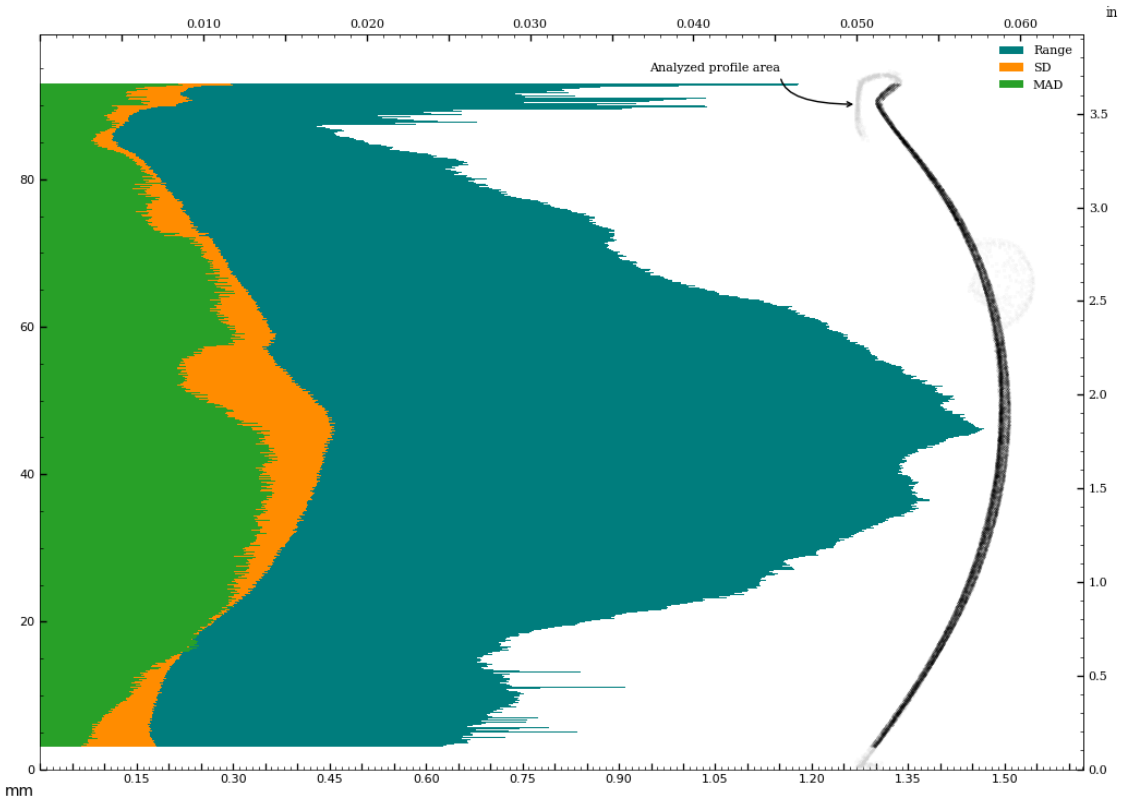

Figure 41: Circularity analysis of exterior samples perpendicular to surface curvature

Circularity analysis of exterior surface - in z-plane

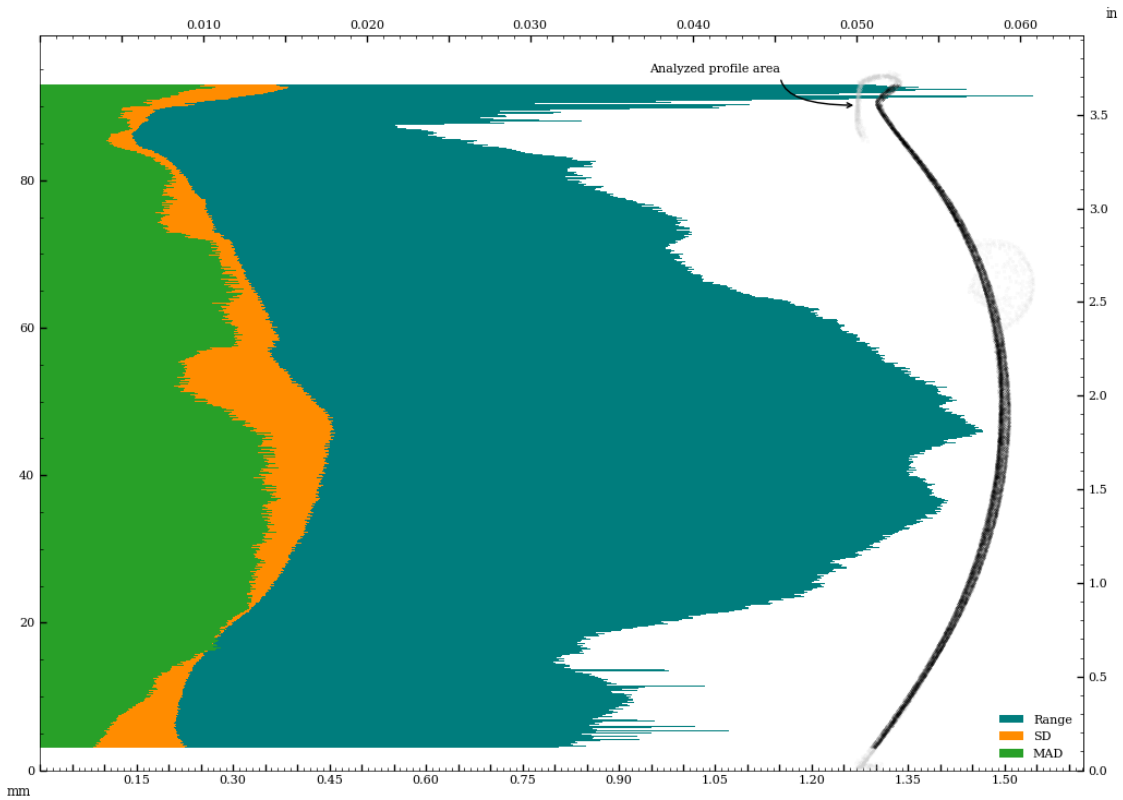

Figure 42: Circularity analysis of exterior surface - in z-plane

Copyright 2025, Stine Gerdes - This work is licensed under CC BY-NC-SA 4.0

Circularity analysis of exterior samples perpendicular to surface curvature

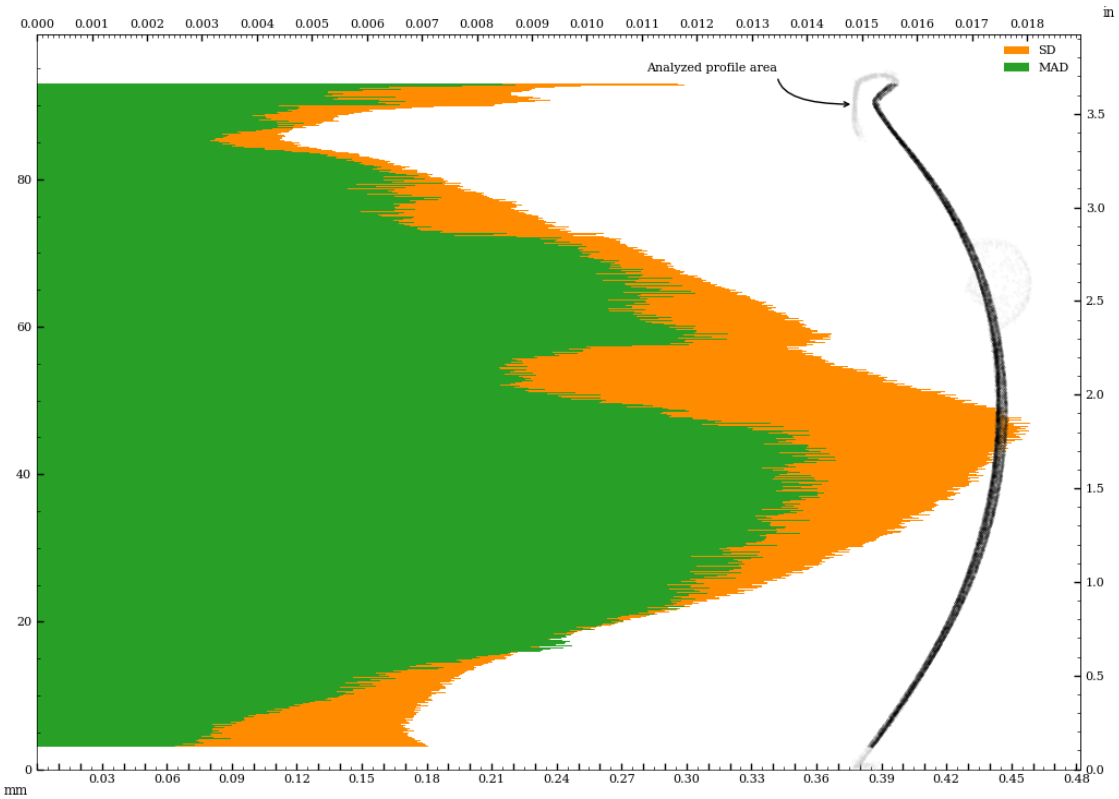

Figure 43: Circularity analysis of exterior samples perpendicular to surface curvature

Circularity analysis of exterior surface - in z-plane

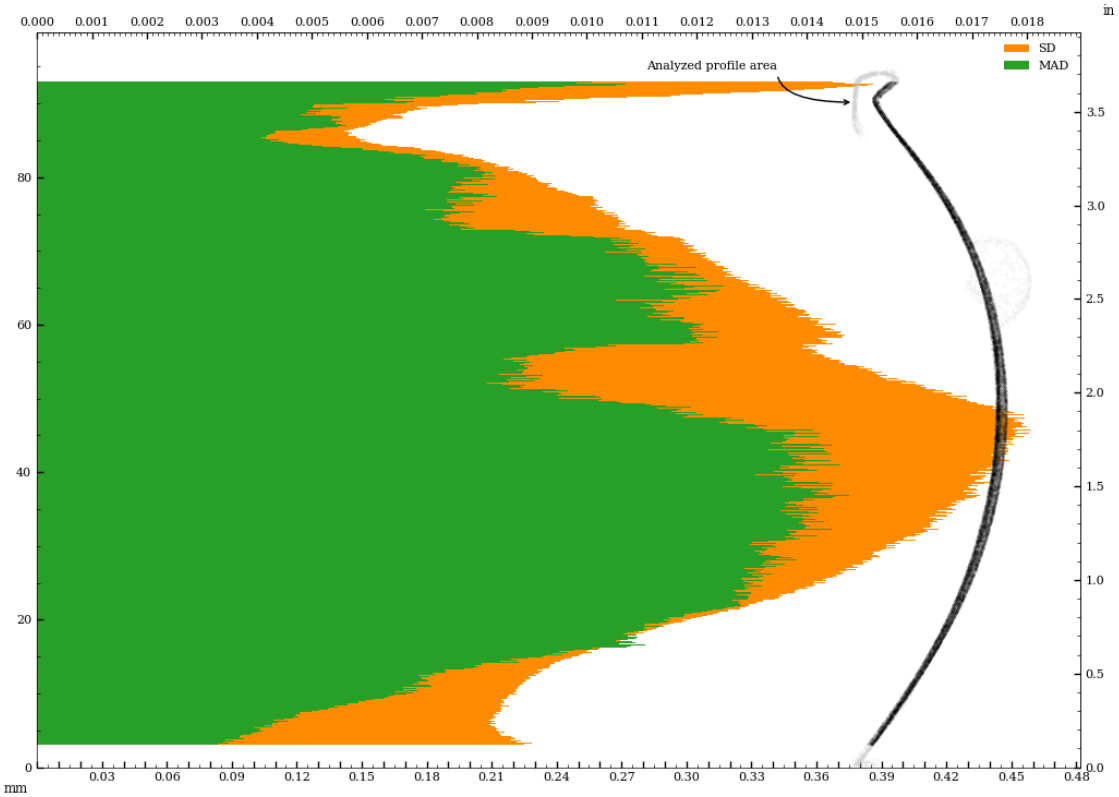

Figure 44: Circularity analysis of exterior surface - in z-plane

Copyright 2025, Stine Gerdes - This work is licensed under CC BY-NC-SA 4.0

Circularity analysis of interior samples perpendicular to surface curvature

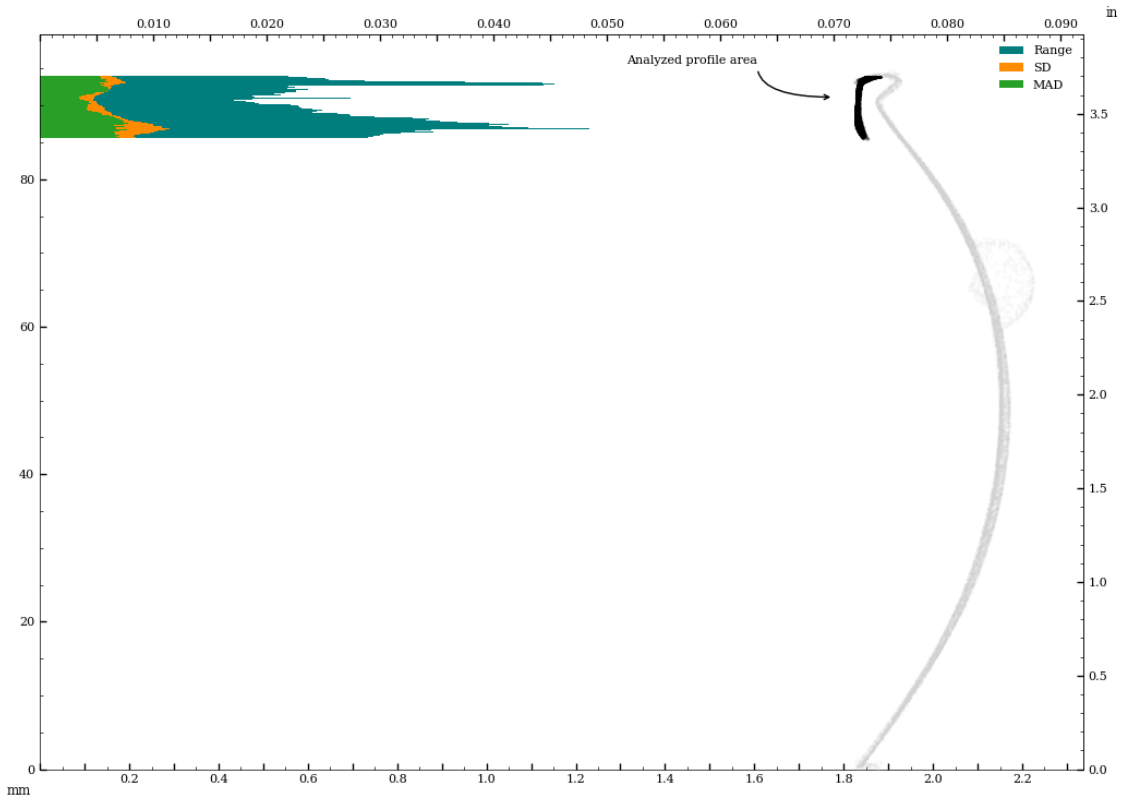

Figure 45: Circularity analysis of interior samples perpendicular to surface curvature

Circularity analysis of interior surface - in z-plane

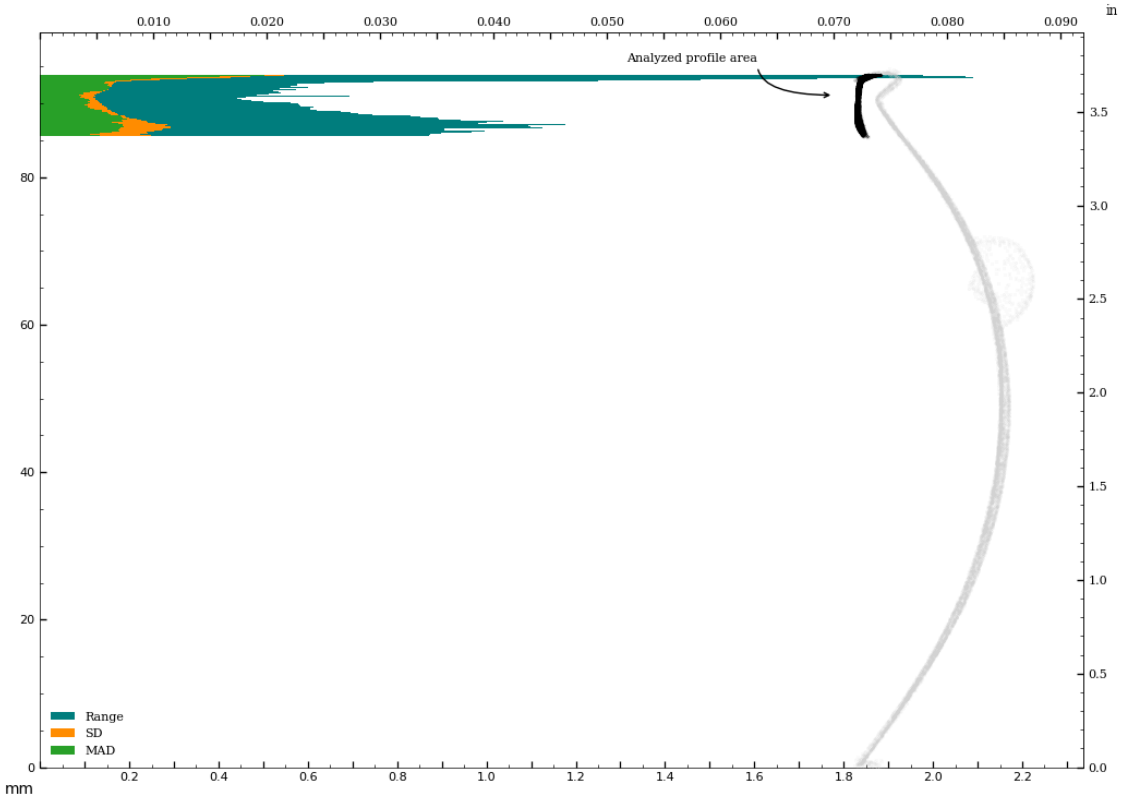

Figure 46: Circularity analysis of interior surface - in z-plane

Copyright 2025, Stine Gerdes - This work is licensed under CC BY-NC-SA 4.0

Circularity analysis of interior samples perpendicular to surface curvature

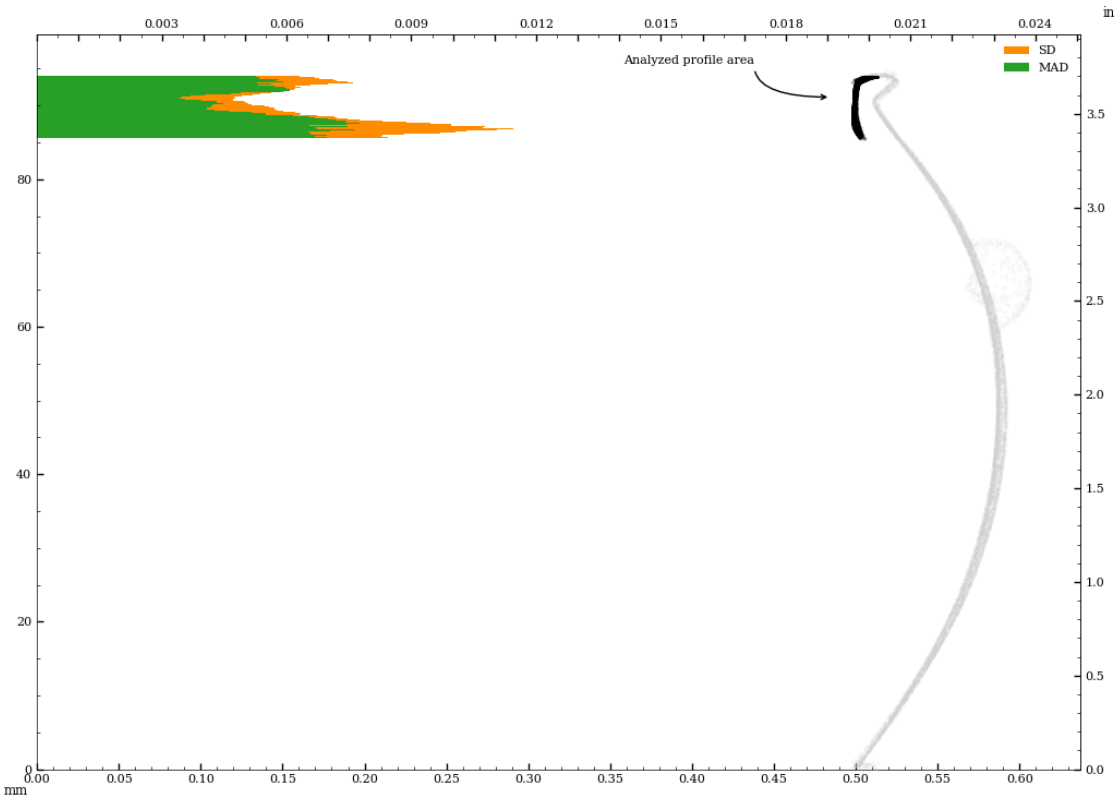

Figure 47: Circularity analysis of interior samples perpendicular to surface curvature

Circularity analysis of interior surface - in z-plane

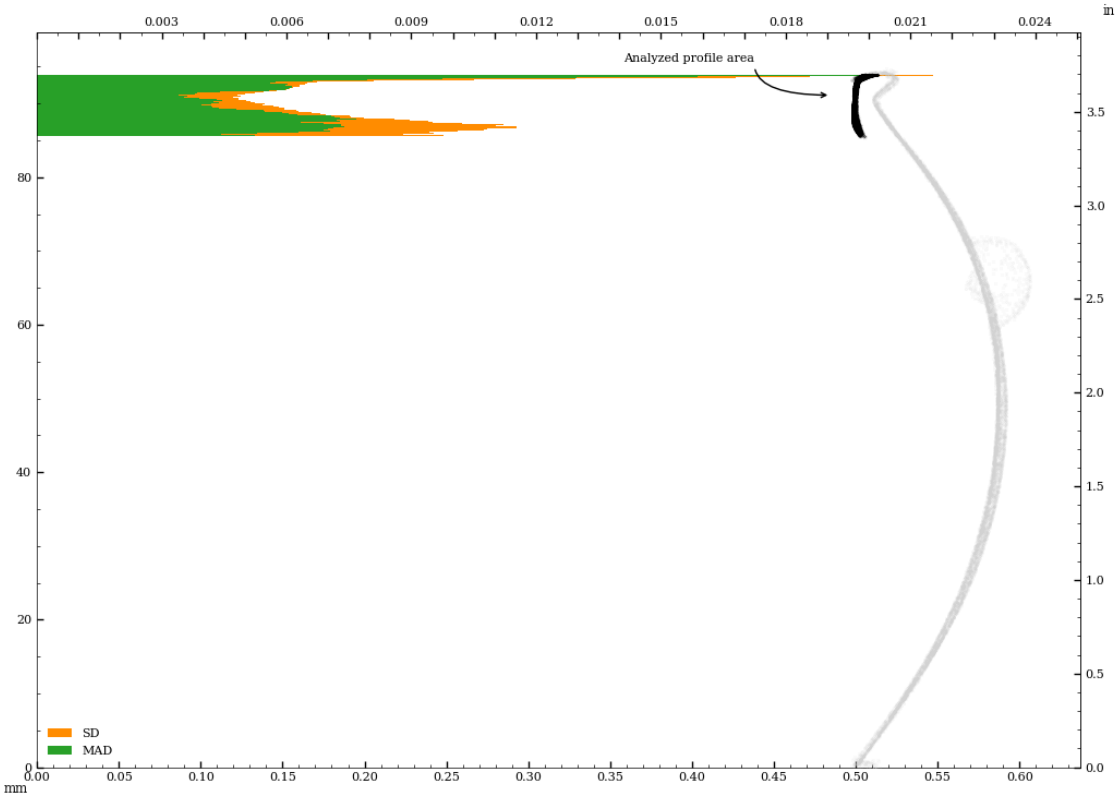

Figure 48: Circularity analysis of interior surface - in z-plane

Copyright 2025, Stine Gerdes - This work is licensed under CC BY-NC-SA 4.0

Appendix B - Comparison Of Concentricity Measurements (Z-plane vs. surface-perpendicular)

Metric

Concentricity measurements perpendicular to surface curvature

Tag	Reference	Deviation	Sample size	Circle fit residuals analysis for sample listed in Tag column						
				Range full	Range inliers	SD full	SD inliers	MAD full	MAD inliers	Center (x,y)
		mm		mm	mm	mm	mm	mm	mm	µm
c01	z-axis	0.076	1079	0.531	0.531	0.139	0.139	0.100	0.100	−17, −74
c02	z-axis	0.028	1688	1.089	1.089	0.331	0.331	0.251	0.251	17, 22
c03	z-axis	0.020	2233	1.464	1.464	0.450	0.450	0.331	0.331	3, −19
c04	z-axis	0.025	1891	1.159	1.159	0.358	0.358	0.313	0.313	−14, 21
c05	z-axis	0.112	1134	0.742	0.742	0.181	0.181	0.143	0.143	108, 32
c06	z-axis	0.223	985	0.690	0.581	0.169	0.161	0.149	0.146	−222, −13
c01	c06	0.214	1079	0.531	0.531	0.139	0.139	0.100	0.100	205, −61

Concentricity measurements in z-plane

Tag	Reference	Deviation	Sample size	Circle fit residuals analysis for sample listed in Tag column						
				Range full	Range inliers	SD full	SD inliers	MAD full	MAD inliers	Center (x,y)
		mm		mm	mm	mm	mm	mm	mm	µm
c01	z-axis	0.105	1496	0.886	0.886	0.227	0.227	0.129	0.129	−29, −100
c02	z-axis	0.008	1749	1.127	1.127	0.340	0.340	0.274	0.274	5, 7
c03	z-axis	0.022	2260	1.437	1.437	0.458	0.458	0.354	0.354	10, −20
c04	z-axis	0.017	2186	1.233	1.233	0.379	0.379	0.326	0.326	−16, −6
c05	z-axis	0.169	1739	1.008	1.008	0.240	0.240	0.155	0.155	165, 40
c06	z-axis	0.223	977	0.708	0.614	0.177	0.170	0.156	0.157	−223, −12
c01	c06	0.213	1496	0.886	0.886	0.227	0.227	0.129	0.129	194, −88

Copyright 2025, Stine Gerdes - This work is licensed under CC BY-NC-SA 4.0

Concentricity measurements perpendicular to surface curvature

Tag	Reference	Deviation	Sample size	Circle fit residuals analysis for sample listed in Tag column						
				Range full	Range inliers	SD full	SD inliers	MAD full	MAD inliers	Center (x,y)
		in		in	in	in	in	in	in	thou
c01	z-axis	0.0030	1079	0.0209	0.0209	0.0055	0.0055	0.0039	0.0039	−0.7, −2.9
c02	z-axis	0.0011	1688	0.0429	0.0429	0.0131	0.0131	0.0099	0.0099	0.7, 0.9
c03	z-axis	0.0008	2233	0.0576	0.0576	0.0177	0.0177	0.0130	0.0130	0.1, −0.8
c04	z-axis	0.0010	1891	0.0456	0.0456	0.0141	0.0141	0.0123	0.0123	−0.5, 0.8
c05	z-axis	0.0044	1134	0.0292	0.0292	0.0071	0.0071	0.0056	0.0056	4.2, 1.3
c06	z-axis	0.0088	985	0.0272	0.0229	0.0066	0.0063	0.0059	0.0057	−8.8, −0.5
c01	c06	0.0084	1079	0.0209	0.0209	0.0055	0.0055	0.0039	0.0039	8.1, −2.4

Concentricity measurements in z-plane

Tag	Reference	Deviation	Sample size	Circle fit residuals analysis for sample listed in Tag column						
				Range full	Range inliers	SD full	SD inliers	MAD full	MAD inliers	Center (x,y)
		in		in	in	in	in	in	in	thou
c01	z-axis	0.0041	1496	0.0349	0.0349	0.0090	0.0090	0.0051	0.0051	−1.2, −4.0
c02	z-axis	0.0003	1749	0.0444	0.0444	0.0134	0.0134	0.0108	0.0108	0.2, 0.3
c03	z-axis	0.0009	2260	0.0566	0.0566	0.0180	0.0180	0.0140	0.0140	0.4, −0.8
c04	z-axis	0.0007	2186	0.0485	0.0485	0.0149	0.0149	0.0128	0.0128	−0.6, −0.3
c05	z-axis	0.0067	1739	0.0397	0.0397	0.0094	0.0094	0.0061	0.0061	6.5, 1.6
c06	z-axis	0.0088	977	0.0279	0.0242	0.0070	0.0067	0.0061	0.0062	−8.8, −0.5
c01	c06	0.0084	1496	0.0349	0.0349	0.0090	0.0090	0.0051	0.0051	7.6, −3.5

Copyright 2025, Stine Gerdes - This work is licensed under CC BY-NC-SA 4.0